GEOLOGICA CARPATHICA, 2025, 76, 5, 369–388 https://doi.org/10.31577/GeolCarp.2025.20

Geochemical constraints on the origin of phonolites from the Lužické hory Mts., Ohře (Eger) Rift, Bohemian Massif

SIMONA KRMÍČKOVÁ[1,2,✉], LUKÁŠ KRMÍČEK[1,2], ZDENĚK ŘANDA[3], JAROMÍR ULRYCH[1], EMIL JELÍNEK[4], LUKÁŠ ACKERMAN[1] and JIŘÍ MIZERA[3]

[1]Czech Academy of Sciences, Institute of Geology, Rozvojová 269, CZ-165 00 Prague 6, Czech Republic
[2]Masaryk University, Department of Geological Sciences, Faculty of Science, Kotlářská 2, CZ-611 37 Brno, Czech Republic
[3]Czech Academy of Sciences, Nuclear Physics Institute, Husinec-Řež 130, CZ-250 68 Řež, Czech Republic
[4]Charles University, Institute of Geochemistry, Mineralogy and Mineral Resources, Faculty of Science, Albertov 6, CZ-128 43 Prague 2, Czech Republic

Dedicated to the memory of Kadosa Balogh († died on October 18, 2016)

(Manuscript received June 1, 2025; accepted in revised form November 7, 2025; Associate Editor: Igor Broska)

Abstract: Geochemical and petrological data are reported for phonolites from the Lužické hory Mts. in the northeastern part of the Ohře (Eger) Rift near the junction with the Lusatian Fault. The rocks are collectively enriched in incompatible trace elements such as Rb, REEs, Zr, Hf, U, Th, Nb, Ta (concentrated mainly in hainite, Nb-rich titanite and aegirine) and volatile components such as F and Cl. On the other hand, the phonolites are significantly depleted in Ti and P and partly also in Sr and Ba contents. The K–Ar dating provided scattered ages in the range from 34 to 27 Ma. Two geochemically different phonolite types were recognized: (i) type A (higher Sr>90 ppm, Ba>130 ppm) having initial $^{87}Sr/^{86}Sr$= 0.7032–0.7094 and ε_{Nd}=2.9–3.4, similar to those phonolites that are predominant in the nearby České středohoří Mts., and (ii) prevailing type B with lower contents of Sr<20 ppm and Ba<60 characterized by a decoupled Sr–Nd systematics (initial $^{87}Sr/^{86}Sr$ ratios up to ~0.714) at narrow ε_{Nd} of 3.2–3.8. Yet, both phonolite types exhibit relatively restricted variations in initial $^{206}Pb/^{204}Pb$ (19.2–19.5), $^{207}Pb/^{204}Pb$ (15.61–15.66) and $^{208}Pb/^{204}Pb$ (39.07–39.30), indicating their derivation from a similar metasomatically enriched mantle source. The observed geochemical characteristics of the studied phonolites can be best explained by (i) variable degree of clinopyroxene and feldspar fractional crystallization from primary basanitic magma, (ii) degree of assimilation-fractional crystallization (AFC) processes during the magma ascent, and/or (iii) late-magmatic to post-magmatic hydrothermal processes related to selective enrichment of some incompatible elements.

Keywords: Cenozoic volcanism, Bohemian Massif, Ohře (Eger) Rift, Lužické hory Mts., phonolite, assimilation-fractional crystallization, Sr–Nd–Pb isotopes

Introduction

Classic examples of Cenozoic phonolites and associated trachytes that formed in extensional tectonic settings can be found in the East-African Rift System (Macdonald 2003; Macdonald & Scaillet 2006 and references therein). Alternatively, they also can originate in ocean island settings, e.g., in the Atlantic Ocean (Tristan da Cunha; Le Roex et al. 1990) and Pacific Ocean (French Polynesia, Marquesas; Legendre et al. 2005). In the Central European Volcanic Province (Dèzes et al. 2004; Binder et al. 2023), felsic volcanic rocks have been reported particularly from the French Massif Central (Briot et al. 1991; Wilson et al. 1995; Bernth et al. 2002), numerous provinces in Germany (Jung 1995; Schreiber et al. 1999; Binder et al. 2024) and the Bohemian Massif (Kühn 1990; Pazdernik 1997, 1998; Ackerman et al. 2015; Büchner et al. 2015, 2024; Ulrych et al. 2016; Wenger et al. 2017).

An important issue in studies of bimodal mafic–felsic association is the origin and the processes leading to generation of phonolite magma. For example, Maciotta et al. (1990) and Vaněčková et al. (1993) have demonstrated the origin of phonolite magma by low-pressure fractional crystallization (mostly of clinopyroxene) from a parental (nephelinitic?) magma at shallow crustal levels. In comparison, two petrogenetic processes were identified in the origin of phonolites from Siebengebirge (Kolb et al. 2012): (i) derivation by partial melting of a mantle source, and (ii) derivation from a similar mantle source with a substantial crustal contamination during the ascent. Le Bas (1987) distinguished two groups of phonolites: (i) Group I associated with alkali basalts and basanites and characterized by low Sr and Ba (<100 ppm) and high Rb contents (>400 ppm) due to extensive plagioclase fractionation, and (ii) Group II with high Sr and Ba contents mostly >1000 ppm and low Rb contents of ca. 10 ppm derived through the crystallization of olivine-poor nephelinite melts. However, a large range from high Sr and high Ba (>1000 ppm) to low Sr (<4 ppm) and low Ba phonolites can erupt at the same time from the same vent, cf. Laacher See phonolites from the East

✉ corresponding author: Simona Krmíčková
krmickova@gli.cas.cz

Eifel volcanic field (Wörner et al. 1983). Wilson et al. (1995) documented a common asthenospheric mantle source for two coexisting strongly alkaline (basanite–tephrite–phonolite) and weakly alkaline (alkali basalt–trachyandesite–trachyte–rhyolite) series in the Cantal, French Massif Central, that originated by a combined assimilation-fractional crystallization process.

The aim of this paper is to compare geochemical signatures and sources of the two predominant phonolite occurrences in the Bohemian Massif – Lužické hory Mts., with those known from the central part of the Ohře (Eger) Rift represented by the volcanic complex of the České středohoří Mts. The phonolites of the Lusatian region significantly expand the geochemically and isotopically defined phonolite groups (types A and B) in the České středohoří Mts. (CS) as described by Ackerman et al. (2015).

Geological setting

The intraplate Central European Volcanic Province (CEVP) extends from Spain across France and Germany to the Czech Republic and southwest Poland. Most of the volcanism is related to a generally SSW–NNE trending rift belt formed in the Early Cenozoic, including, e.g., Limagne Graben, Rhone Graben, Upper Rhine Graben, Lower Rhine depression, Leine Graben and Rhenish Shield, where it splits and continues NW to the Lower Rhine Graben and NE to the Ohře (Eger) Rift (Ziegler 1994; Dèzes et al. 2004; Lustrino & Wilson 2007; Meyer & Foulger 2007). The main Cenozoic volcanic areas in France and Germany are associated with an E–W trending older suture zone in the Variscan basement, resulting in an E–W belt of generally N–S trending graben structures (Lustrino & Wilson 2007). This major-scale European Cenozoic rift system (ECRIS) formed in response to the Alpine orogeny caused by the collision of European and African plates in Early Tertiary time (Ziegler 1994; Dèzes et al. 2004). The Alpine orogeny-related passive asthenospheric mantle upwelling resulted in a generation of the large volume of mantle-derived alkaline magmas by decompression melting of both asthenospheric and lithospheric sources with minor crustal contamination (Wilson & Downes 1991; Ulrych et al. 2000a, 2011; Jung et al. 2013; Pfänder et al. 2018; Krmíčková et al. 2020). On the basis of a comprehensive review of major, trace element and Sr–Nd–Pb isotope data, a rather common sub-lithospheric mantle source component was identified for the whole region (Lustrino & Wilson 2007).

Although the Cenozoic volcanism of the CEVP is commonly considered the first major intraplate event since the Permo–Carboniferous collapse of the Variscan orogen (Wilson & Downes 1991), earlier extension-related magmatism occured at scattered localities already during the Late Mesozoic. Early Cretaceous alkaline volcanic rocks are documented, e.g., from the North Pyrenean region, Alps, Western Carpathian nappes or the Mecsek Mts. in the Pannonian area (Harangi 1994 and references therein). These occurrences differ in geodynamic setting, age and lithological associations from the Cenozoic CEVP volcanism, but they highlight that alkaline magmatism recurred in Central and Western Europe throughout post-Variscan times. It should be noted that the Carpathian–Pannonian region, although also characterized by diverse Cenozoic volcanism related to lithospheric thinning and asthenospheric upwelling, is not considered a part of the CEVP or ECRIS systems, as major rift structures are absent (e.g., Harangi & Lenkey 2007; Lexa et al. 2010; Szakács et al. 2018; Harangi et al. 2026).

The Lužické hory Mts. represent a continuation of the CS to the NE segment arm of the Ohře (Eger) Rift. It forms an about 20 km long and 15 km wide range of isolated phonolitic and basaltic plugs and pipes exposed by denudation; preserved relics of surficial volcanic products occur rarely as fillings of diatremes and phonolitic and basaltic lava flows (Büchner et al. 2015). Nevertheless, the Cenozoic volcanism in the northern part of the Ohře (Eger) Rift is concentrated to the area of its junction with the NW–SE striking Lusatian Fault (Coubal et al. 2014; Ulrych et al. 2022). The peak of volcanic activity in the Ohře (Eger) Rift culminated in the Middle Oligocene to Lower Miocene at ~30 to 24 Ma (Ziegler 1994; Ulrych et al. 2011; Krmíček et al. 2021). Similarly, the Ar–Ar ages of basaltic and phonolitic rocks of the Lusatian Volcanic Field given by Büchner et al. (2015) range from 35 to 27 Ma.

Phonolitic and trachytic rocks make up ~8 vol.% of all Tertiary volcanic rocks in the CS (Hibsch 1930), but up to 50 vol.% of the present-day surface volcanic occurrences in the Lužické hory Mts. (Kühn 1990; Ulrych & Pivec 1997).

Analytical methods

The study of phonolites of the Lužické hory Mts., emerging as a higher block of the Ohře (Eger) Rift, followed up on the research of phonolites of the České středohoří Mts. (Ackerman et al. 2015). In the Lužické hory Mts. region, around 30 significant phonolite localities are known in Bohemia (Kühn 1990). Büchner et al. (2015) reported the presence of phonolites also from adjacent Lusatia (Germany). A total of ten fresh rock specimens (0.5–5 kg) from nine characteristic occurrences (quarries and natural outcrops) in northern Bohemia were chosen for the geochemical research (Fig. 1). From each of selected samples, polished thin sections were prepared for the optical microscopy and electron probe microanalysis (EPMA). Furthermore, the samples were crushed into 1–2 cm pieces free of xenoliths and altered parts. These samples were again crushed (<2 mm) and pulverized to a fine analytical fraction (<0.125 μm) in an agate mill. The powders were then subjected to geochemical analyses of major oxide, trace element and radiogenic isotope compositions.

The mineral analyses of two phonolite samples were carried out using a Cameca SX-100 electron microprobe at the Institute of Geology of the Czech Academy of Sciences with a beam diameter of 10 μm, an accelerating voltage of 15 kV, a beam current of 10 nA, and a counting time of 10 s for all

elements. Concentrations of the following elements were determined (standards, spectrometer crystals and measured lines are given in parentheses): Si (diopside, forsterite, wollastonite, titanite, andradite; LTAP; *Kα*), Ti (rutile, titanite, anatase, TiO; LPET; *Kα*), Zr (zircon; LPET; *Lβ*), Al (jadeite, spessartine, sanidine, andalusite; LTAP; *Kα*), Cr (chromite, CrO; LPET; *Kα*), Mg (periclase, pyrope; LTAP; *Kα*), Ca (diopside, wollastonite; LPET; *Kα*), Mn (rhodonite, spessartine; LIF; *Kα*), Fe (haematite, almandine; LIF; *Kα*), Na (jadeite, albite; LTAP; *Kα*), K (sanidine, orthoclase; LPET; *Kα*), F (fluorite, topaz; PC0; *Kα*) and Cl (tugtupite, vanadinite; LPET; *Kα*). The detection limits of the measured elements ranged from 99 to 948 ppm. Data reduction was performed using X-PHI correction (Merlet 1992).

Whole-rock major element concentrations in phonolites (10 samples) were determined at the Institute of Geochemistry, Mineralogy and Mineral Resources, Faculty of Science, Charles University, using wet chemical methods that basically followed those described in detail by Johnson & Maxwell (1981) and Potts (1995). The accuracy of the method was monitored through the periodical analyses of the reference materials SY-4 (CCRMP) and AGV-2 (USGS), both yielded a total error of ±5 % with respect to certified/recommended values. The trace element analyses of the whole-rock samples were carried out after modified total digestion in acids (HF+$HClO_4$) and fusion (Na_2CO_3+$Na_2B_4O_7$) in platinum crucibles followed by the ICP–MS (VG PQ3, iCAP Q) using the analytical protocol and calibration strategy closely followed those described in Strnad et al. (2005). The precision of the analyses was better than 5 %, while the accuracy estimated through the analyses of the reference materials AGV-2 and BCR-2 (USGS) varied between ~5 and 10 %.

Instrumental neutron and photon activation analyses (INAA and IPAA), performed at the Nuclear Physics Institute of the Czech Academy of Sciences, were employed for quality control at the same 10 rock samples, and to complement the whole-rock analyses of phonolites (concentrations of Cl and F in Table 1; Supplementary Material S2). For INAA, the LVR-15 nuclear reactor within the CANAM infrastructure (project No. LM2011019 of the Ministry of Education) was employed. Irradiations for IPAA employed high-energy photons (*bremsstrahlung*) produced in the microtron MT-25 (cyclic electron accelerator). Various modes of INAA and IPAA were applied. Experimental details including the list of determinable elements and associated uncertainties have been described in Řanda et al. (2007) or Mizera & Řanda (2010). Fluorine was determined using a non-destructive IPAA method described in Krausová et al. (2015). For the quality control of analytical data, the USGS AGV-1 (andesite) and USGS GSP-2 (granodiorite) reference rock materials were simultaneously analysed.

The K–Ar ages of two phonolite samples were measured at the Institute of Nuclear Research of the Hungarian Academy of Sciences. The geochronology methodology on matrix of rock samples followed the procedures described by Balogh (1985), and results of an interlaboratory calibration have been presented by Odin (1982). Standards LP-6 and HD-B1 have been used for calibration of the measurement of ^{40}Ar(rad) and K concentrations. Argon isotope ratios have been calibrated by atmospheric Ar, accepting 295.5 for the $(^{40}Ar/^{36}Ar)_{atm}$.

The Sr–Nd–Pb isotope compositions of 10 unaltered phonolite samples (fresh rocks with very low CO_2 contents) were acquired at the Institute of Geology of the Czech Academy of Sciences, using the protocol described in detail by Ackerman et al. (2020) and Krmíček et al. (2020). The decomposition of samples in a mixture of 23 M HF and 7 M HNO_3 for 72 hours on a hot plate at 140 °C was followed by the element separation from the matrix using the slightly modified scheme of Pin et al. (2014). Strontium and Pb were isolated by a Sr resin (TrisKem) using 2 ml of 0.05 M HNO_3 and 6 M HCl, respectively. In comparison, a combination of TRU and LN resins (TrisKem) was used for Nd isolation using 0.25 M HCl. The isotope analyses of Sr, Nd and Pb were carried out on a Thermo Triton Plus thermal ionization mass spectrometer (TIMS). In case of Sr, the samples were analyzed on W filaments in the presence of Ta activator, whereas Nd and Pb were analyzed on Re filaments using a double and single configuration, respectively. The instrumental mass bias during Pb analyses was corrected using the long-term analyses of NIST SRM 981 reference material applying an average mass fractionation factor of 0.136 ‰ per mass unit relative to the reference values (Todt et al. 1996). The accuracy of the whole procedure was monitored through the repeated analyses of a BCR-2 (USGS) reference material with obtained values similar to those previously published (Jochum & Nohl 2008).

Results

Petrography

Phonolites from nine representative localities in the Lužické hory Mts. area were studied. Locations of the sampling sites are shown in Fig. 1, their geographical coordinates are given in Table 1, and examples of two sampled outcrops (Klíč and Sokol near Petrovice) are displayed at Fig. 2A, B. Electron microprobe analyses of representative rock-forming and accessory minerals are summarized in Supplementary Material S1.

The phonolite samples are greenish-grey to dark grey in colour, (micro)porphyritic with fine-grained to aphanitic holocrystalline groundmass (Fig. 2C, D). The rocks have rarely glassy, trachytic texture (e.g., Klíč Hill; Fig. 2E), and are occasionally greasy in appearance with increased nepheline content. Groundmass consists of abundant alkali feldspar (sanidine and anorthoclase; see Supplementary Material S1A) with rare interstitial plagioclase, feldspathoids, and minor mafic minerals. The phenocrysts are represented by alkali feldspars (sanidine and anorthoclase; see Supplementary Material S1A), feldspathoids of the sodalite group (see Supplementary Material S1B), rare interstitial nepheline and microphenocrysts of clinopyroxene (aegirine to aegirine-augite; see Supplementary Material S1C) substantially prevailing over

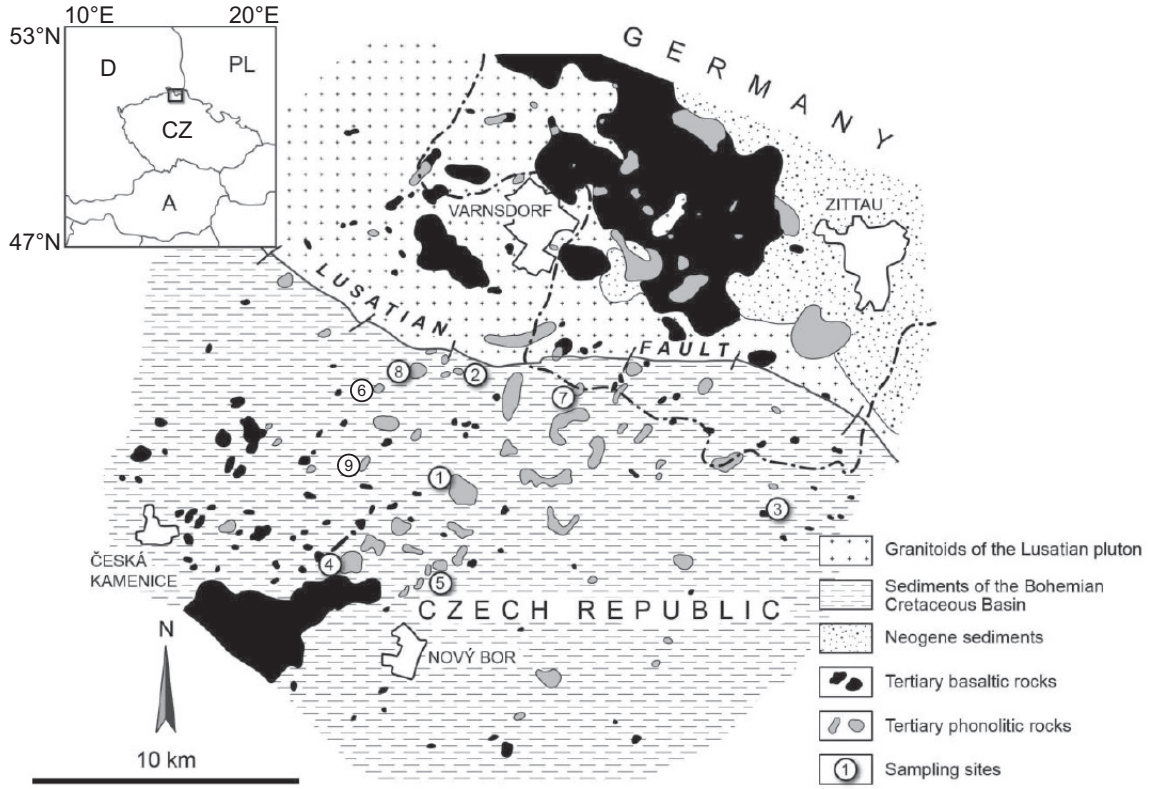

Fig. 1. A simplified geological map of the Lužické hory Mts. (after Kühn 1990) showing the localities of phonolitic rocks and the sampling sites. Numbers of sampling sites correspond to numbering of analyses in Tables 1 and 3.

Table 1: Major oxide, trace element, and CIPW normative composition of phonolites from the Lužické hory Mts.

No.	**1**	**2**	**3A**	**3B**	**4**	**5**	**6**	**7**	**8**	**9**
Sample	**NBPH1**	**NBPH2**	**16PH1**	**NBPH3**	**NBPH4**	**NBPH5**	**16PH4**	**NBPH7**	**NBPH8**	**16PH5**
Rock type	PH-B	PH-B	PH-B	PH-B	PH-A	PH-A	PH-A	PH-B	PH-A	PH-B
Locality	Velký Buk, Svor	Tolštejn, Jiřetín pod Jedlovou	Sokol, Petrovice	Sokol, Petrovice	Polevský vrch, Polevsko	Klíč, Svor	Malý Stožec, Rybniště	Luž, Mařenice	Jedlová, Jiřetín pod Jedlovou	Sokol, Kytlice
Latitude (N)	50°48.993'	50°51.429'	50°48.399'	50°48.478'	50°47.514'	50°47.313'	50°51.056'	50°50.916'	50°51.459'	50°49.335'
Longitude (E)	14°35.365'	14°34.965'	14°44.959'	14°45.020'	14°31.347'	14°34.145'	14°32.425'	14°38.799'	14°33.697'	14°31.847'
SiO_2 [wt.%]	60.69	54.92	58.97	54.82	59.86	58.85	57.28	58.38	56.78	59.86
TiO_2	0.24	0.16	0.21	0.20	0.39	0.19	0.31	0.17	0.27	0.20
Al_2O_3	19.02	21.02	19.53	19.17	18.98	21.05	20.85	20.90	20.94	19.95
Fe_2O_3	2.08	2.24	2.57	2.40	2.38	1.47	2.74	2.02	2.34	2.39
FeO	0.29	0.18	0.12	0.18	0.72	0.43	0.53	0.39	0.56	0.16
MgO	0.13	0.22	0.06	2.91	0.18	0.06	0.16	0.04	0.09	0.13
CaO	1.45	0.80	0.95	1.65	1.75	0.70	1.84	0.70	1.60	1.03
MnO	0.30	0.30	0.66	0.53	0.19	0.20	0.21	0.16	0.21	0.29
Na_2O	8.09	10.8	8.39	6.50	7.29	9.60	7.91	10.2	9.46	7.85
K_2O	5.26	4.92	5.13	4.83	5.58	5.61	6.36	5.66	5.46	5.62
P_2O_5	0.02	0.02	0.02	0.02	0.07	0.06	0.03	0.04	0.11	0.03
H_2O^+	1.74	3.82	0.44	4.56	2.32	1.19	0.12	0.66	1.70	0.1
H_2O^-	0.67	0.63	1.96	1.98	n. d.	n. d.	1.22	n. d.	n. d.	1.68
CO_2	n. d.	n. d.	0.18	n. d.	0.10	0.10	0.13	0.20	0.10	0.11
Total	99.98	100.06	99.19	99.75	99.81	99.51	99.69	99.52	99.62	99.40
F [ppm]	531	1078	n. d.	290	374	1686	n. d.	870	1802	n. d.
Cl	1740	2955	n. d.	677	230	4100	n. d.	3975	5715	n. d.
Sc	0.71	1.1	0.71	0.55	0.75	0.23	0.21	0.62	0.95	0.52
V	3.6	10	1.7	5.1	15	13	13	11	20	8.6

Table 1 (continued)

No.	1	2	3A	3B	4	5	6	7	8	9
Sample	NBPH1	NBPH2	16PH1	NBPH3	NBPH4	NBPH5	16PH4	NBPH7	NBPH8	16PH5
Cr	2.1	1.7	2.7	3.0	0.61	0.98	0.64	1.6	0.49	1.5
Co	0.11	0.29	0.16	0.20	0.42	0.26	0.28	0.22	0.45	0.34
Ni	0.88	0.82	3.5	3.2	0.36	0.62	0.47	1.69	0.30	0.72
Rb	310	385	474	458	161	201	179	299	255	229
Sr	1.6	38	9.5	6.8	231	86	493	3.6	152	53
Ba	6.1	37	13	8.9	852	129	1881	5.3	207	60
Y	53	40	12	15	16	12	16	9.7	19	26
Zr	1571	2715	3037	2950	372	1023	646	1384	587	1175
Nb	480	348	937	928	207	131	170	110	189	278
La	195	204	202	221	111	85	114	85	124	165
Ce	300	256	357	348	161	112	155	81	152	211
Pr	24	17	30	29	12	7.0	12	4.6	11	14
Nd	62	38	80	83	29	16	29	8.8	26	31
Sm	7.5	4.2	12	12	3.3	1.7	2.9	0.81	3.5	3.0
Eu	1.2	0.80	1.6	1.7	0.80	0.40	0.79	0.15	0.73	0.52
Gd	6.3	3.8	10	13	4.0	1.2	1.9	0.83	4.1	2.5
Tb	1.1	0.64	2.1	2.1	0.46	0.21	0.32	0.13	0.48	0.42
Dy	7.1	4.5	15	15	2.4	1.5	2.1	0.98	2.5	2.9
Ho	1.7	1.1	3.3	3.3	0.54	0.34	0.49	0.26	0.59	0.75
Er	5.7	4.4	11	12	1.8	1.3	1.7	1.1	2.1	2.9
Tm	0.97	0.82	1.9	1.9	0.31	0.23	0.30	0.23	0.37	0.54
Yb	6.9	6.7	13	13	2.4	1.8	2.3	2.0	2.9	4.1
Lu	1.1	1.2	2.0	2.0	0.39	0.32	0.38	0.38	0.50	0.71
Ta	21	5.2	43	41	12	2.4	4.7	1.8	7.3	9.2
Hf	29	39	56	57	11	15	10	20	16	20
Th	50	83	78	76	22	22	19	38	44	38
U	13	24	23	24	6.6	8.3	4.9	12	13	10
Pb	29	44	48	52	14	16	13	24	22	20
Cs	5.0	6.6	9.3	9.3	2.2	2.8	2.4	4.4	4.2	3.7
Zn	221	305	378	381	104	127	106	125	165	148
Cu	1.0	1.0	0.68	0.78	1.7	0.54	0.38	1.0	2.8	0.63
A. I.	1.00	1.10	0.99	0.83	0.95	1.04	0.95	1.10	1.03	0.95
Mg#	10	15	4	69	10	6	9	3	6	9
K/Rb	141	106	89.8	87	287	232	294	157	178	204
Rb/Sr	190	10.2	49.9	44.4	0.70	2.33	0.36	82.6	1.68	4.33
Th/U	3.87	3.45	3.36	3.26	3.31	2.62	3.97	3.24	3.54	3.71
Zr/Hf	53.7	69.1	53.9	53.8	33.2	67.3	61.7	68.9	36.9	59.0
Nb/Ta	22.5	67.6	21.9	24.7	16.6	55.7	35.8	61.8	25.9	30.1
ΣREE	621	543	741	769	330	229	322	186	330	439
La_N/Yb_N	19.0	20.4	10.2	11.8	31.8	31.3	33.6	28.5	29.0	26.9
Eu/Eu*	0.54	0.61	0.44	0.39	0.68	0.87	1.05	0.56	0.59	0.58
Gd/Gd*	1.26	1.20	1.28	1.70	1.50	0.93	0.84	1.35	1.59	1.23
Ba/Nb	0.01	0.11	0.01	n. d.	4.12	0.98	11.1	0.05	1.09	0.22
Zr/Nb	3.27	7.80	3.24	3.25	1.80	7.81	3.81	12.6	3.10	4.23
Zr/Y	29.7	67.8	255	25.0	22.8	86.7	40.2	142	30.5	45.9
CIPW normative composition										
Or	31.1	29.1	30.3	28.5	33.0	33.2	37.6	33.5	32.3	33.2
Ab	54.1	29.6	48.3	47.1	52.9	38.4	32.9	34.2	36.8	46.9
An	0.00	0.00	0.48	0.00	0.00	0.00	2.60	0.00	0.00	2.60
Ne	7.79	27.7	12.3	4.30	4.76	20.9	18.5	22.7	22.0	10.6
Ac	0.00	6.48	0.00	0.00	0.00	3.70	0.00	5.85	2.41	0.00

PH-A = type A phonolite; PH-B = type B phonolite.

Concentrations of Cl and F were determined by INAA and IPAA (instrumental neutron and photon activation analyses), respectively.

A. I.=(Na+K)/Al (alkalinity index); Mg#=100×Mg/(Mg+Fe^{tot}); n. d.=not determined.

* Eu and Gd anomalies were calculated as the ratio between normalized (N) values of Eu or Gd and their interpolated values according to McLennan (1989): $Eu/Eu^*=Eu_N/(Sm_N\times Gd_N)^{0.5}$; $Gd/Gd^*=Gd_N/(Eu_N\times Tb_N)^{0.5}$.

CIPW norm calculation is adopted from Hutchison (1974, 1975): Or=orthoclase; Ab=albite; An=anorthite; Ne=nepheline; Ac=acmite (an obsolete name for aegirine).

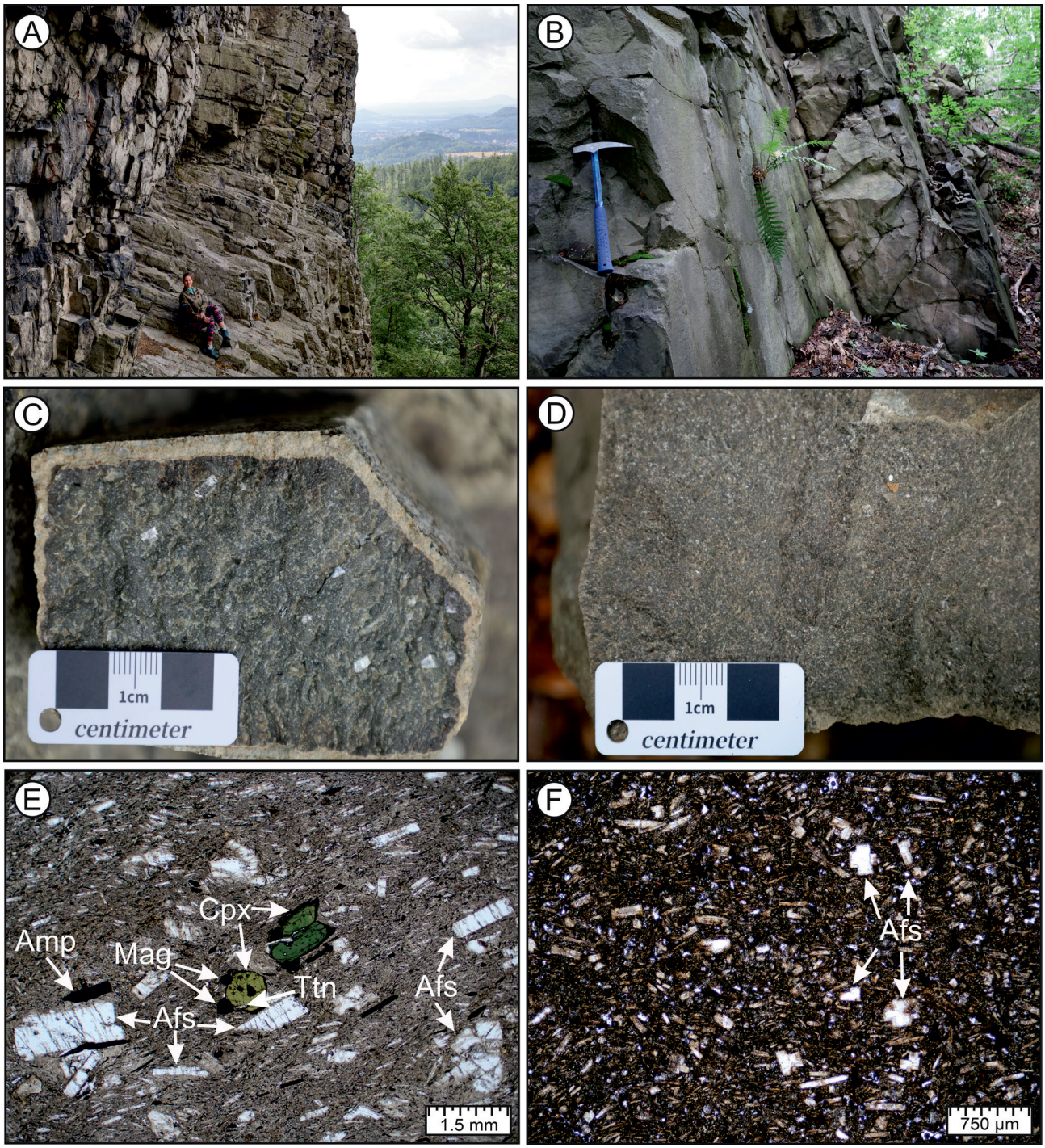

Fig. 2. Field appearance of the phonolite outcrops, megascopic overview of the samples, and texture microphotographs of type A phonolite from Klíč Hill and type B phonolite from Sokol Hill near Petrovice. Abbreviations of the rock-forming minerals are according to Warr (2021). PPL = plane polarized light. **A** — Spectacular phonolite exposure with distinct columnar jointing at Klíč Hill. **B** — Old phonolite quarry at the southern slope of the Sokol Hill near Petrovice. **C** — Type A phonolite sample from Klíč Hill with large phenocrysts of alkali feldspar. **D** — Microporphyritic texture of type B phonolite from Sokol Hill near Petrovice. **E** — Twinned phenocrysts of alkali feldspar and clinopyroxene in trachytic groundmass of flow-oriented thin feldspar laths, and minor magnetite and amphibole almost completely opacitized (PPL; Klíč Hill). **F** — Microphenocrysts of alkali feldspar, occasionally forming cross-shaped twins, in very fine-grained trachytic groundmass (PPL; Sokol Hill near Petrovice).

amphibole. Feldspar (micro)phenocrysts are often characterized by carlsbad twinning, ocassionally even forming right-angled crosses (Fig. 2E, F). Magnetite, titanite, hainite and apatite together with zeolites represent accessories. Zeolites are predominantly of secondary character. Filling of cavities and veins are also present to a limited extent. Other secondary phases are represented mainly by clay minerals, calcite or chlorite (Kühn 1990). Glass is rare because the groundmass of most samples appears to have almost completely crystallized during the cooling and/or because all glass was easily altered to secondary mineral products. It is difficult to estimate the volume fraction of original volcanic glass and its alteration products in clusters of fine components in the groundmass, and the extrusive forms of phonolites with preserved volcanic glass in the Lužické hory Mts. are rare (Shrbený 1989). The crystallization development of the Lužické hory Mts. phonolites can be best compared with the analogous phonolites of the České středohoří Mts. presented by Ackerman et al. (2015). Based on the observed petrography, sequence of crystallization of the mineral phases proceeded primarily in three stages: (i) early magmatic stage represented by rare (micro)phenocrysts of feldspars (anorthoclase to sanidine), feldspathoids (nepheline, sodalite), pyroxene (aegirine to aegirine–augite), amphibole and Ti-magnetite, (ii) main magmatic stage dominated by groundmass consisting of felsic minerals, (rare relic) glass, feldspars (anorthoclase, sanidine, oligoclase to andesine), sodalite, aegirine–augite and Ti-magnetite, and (iii) late-magmatic to post-magmatic stage associated with the massive formation of hydrous minerals such as analcime, and activity of residual fluids rich in Zr–Nb–REE–Ti concentrated in hainite, Nb-titanite, apatite and aegirine.

Main rock-forming minerals

Alkali feldspars represented by anorthoclase and sanidine (Fig. 3A) are the most abundant, partly with elevated An component (2–7 mol.%; see Supplementary Material S1A). They have the character of laths in the microphenocrysts (e.g., Klíč and Sokol near Petrovice hills) and in the groundmass (e.g., Tolštejn Hill). Anhedral feldspar grains and subhedral feldspars laths in the groundmass are often flow-related.

Plagioclase was detected in the form of laths as microphenocrysts in phonolites of Klíč, Polevský vrch and Velký Buk hills only. Subhedral relics of oligoclase to andesine composition are rimmed by alkali feldspar (Kühn 1990).

Feldspathoids/zeolites occur in the form of microphenocrysts in most phonolite samples and contribute to the groundmass to a variable ratio. Their chemical compositions are listed in Supplementary Material S1B. ***Nepheline*** forms small euhedral columnar microphenocrysts (Ks component of 10–15 mol.%) or their partly resorbed relics scattered in the groundmass. It was partly converted to analcime or to a mixture of clay minerals and zeolites. Relics of nepheline phenocrysts correspond mostly to the Si-poor type. Nepheline grains in the groundmass tend to be the Si-rich types formed from the melt as a metastable product of high fractionation during the final stages of crystallization (Dollase & Thomas 1978). Both types of nepheline correspond to the ideal composition of natural nepheline *sensu* Dollase & Thomas (1978). ***Sodalite*** is abundant in the phonolites of Klíč, Luž, Jedlová and Tolštejn hills (characterized by high Cl contents). Euhedral and subhedral isometric sodalite microphenocrysts typically show lobate rims as a result of groundmass resorption. Clusters of sodalite microphenocrysts occur in the phonolites of

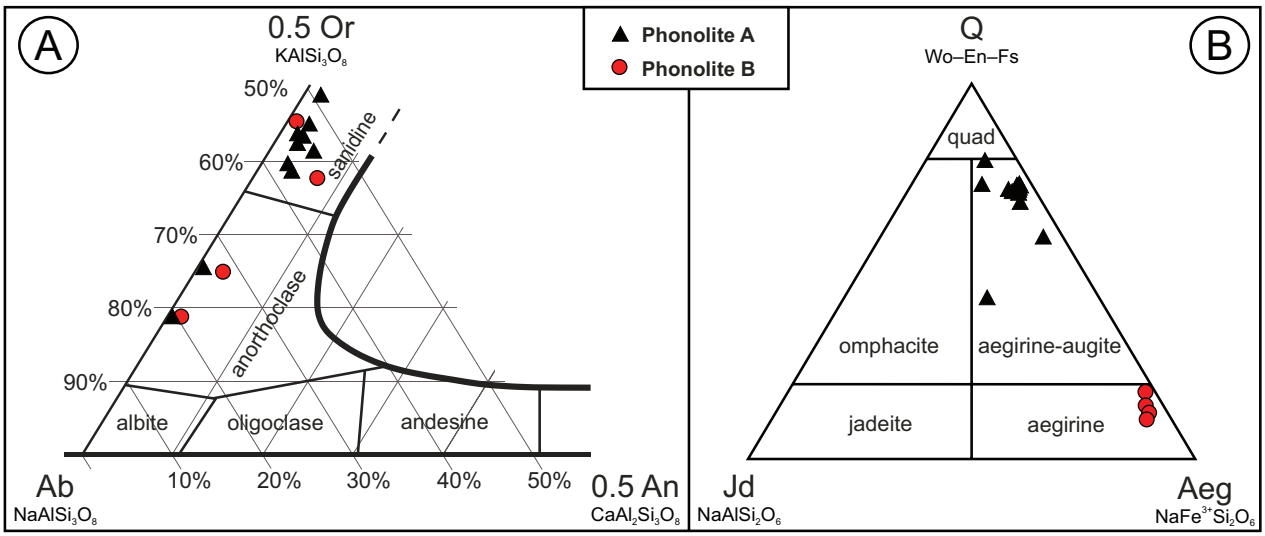

Fig. 3. Chemical compositions of feldspars and clinopyroxene in phonolite samples from Klíč (NBPH5; type A) and Tolštejn (NBPH2; type B) hills. Abbreviations of mineral end members are according to Warr (2021). **A** — Simplified ternary diagram showing alkali feldspars of prevailing sanidine and anorthoclase composition. **B** — Analyses of Ca–Na clinopyroxenes from the type A phonolite plot into the aegirine field, whereas those from the type B phonolite correspond mainly to aegirine-augite in the classification diagram of Morimoto et al. (1988). Q (quad)=Ca–Mg–Fe 'quadrilateral' pyroxenes.

Malý Stožec and Luž hills. Isometric anhedral grains are commonly unevenly distributed in the groundmass. ***Haüyne*** occurs rarely in the cores of sodalite grains or in the form of discrete euhedral microphenocrysts with calcite rims in phonolite of Malý Stožec Hill. ***Analcime*** is present as an independent interstitial phase in the groundmass but also in pseudomorphs after sodalite and nepheline.

Clinopyroxene occurs in the form of subhedral to euhedral microphenocrysts, often prismatic in shape, max. 3 mm in length. In the groundmass, subhedral to euhedral, partially resorbedgrains, max. 0.3 mm in size, and their aggregates are elongated parallel to the fluidal structure (e.g., Velký Buk Hill). Skeletal clinopyroxene development was observed in phonolite from Tolštejn Hill. Composition of clinopyroxene phenocrysts in the type A phonolite (Klíč Hill) corresponds to ***aegirine–augite***, showing only negligible chemical variations between cores and rims, whereas the type B phonolite (Tolštejn Hill) contains phenocrysts of ***aegirine*** (classification of Morimoto et al. 1988; see Fig. 3B and Supplementary Material S1C). ***Aegirine–augite*** is present also in the form of needles in the type A phonolite groundmass.

Amphibole occurs rarely in the form of columnar subhedral to euhedral microphenocrysts (0.1 to 0.5 mm). Intensive transformation of amphibole (opacitization) starts with characteristic magnetite rims (e.g., Klíč Hill; Kühn 1990).

Zirconium silicate ***hainite*** has been originally described from phonolite of Chlum Hill (Hoher Hain) by Blumrich (1883). It is present in the groundmass and in the form of needles in miarolitic cavities of zirconium-rich phonolites, e.g., from Klíč, Tolštejn or Sokol near Petrovice hills (Ulrych et al. 1992; Skála et al. 2010; Supplementary Material S1D). Kühn (1990) reported rims of zirconium silicate ***vlasovite*** around ***hainite*** tabular crystals from the Luž phonolite. High fluorine contents (5.6 to 9.1 wt.%) together with impregnations of ***fluorite*** around ***fluorian eudialyte*** in the groundmass of the Zr-richest phonolite (2650 ppm) from Sokol Hill were reported by Ulrych et al. (1992).

Titanian magnetite is present in the groundmass or in the form of small subhedral microphenocrysts in all phonolite samples. It belongs to the haematite–ilmenite solid solutions series, showing minor variations in TiO_2 contents (5.7–8.7 wt.%; Supplementary Material S1D; Kühn 1990). Contents of MnO are partly higher (2.8–5.5 wt.%; Supplementary Material S1D).

Apatite [chlorapatite/apatite-(CaCl); Kühn 1990] and ***titanite*** belong to the common accessories of the phonolites, forming also clusters with titanian magnetite and aegirine–augite. Titanite shows slightly elevated content of FeO^{tot} (3.8 wt.%; Supplementary Material S1D).

Bulk rock major and trace element characteristics

Major and trace element compositions of the studied phonolites from the Lužické hory Mts. are given in Table 1. Two geochemically different phonolite types were recognized with respect to Sr and Ba contents – type A (high Sr and Ba) and type B (low Sr and Ba).

The rocks plot mainly into the phonolite field in the TAS (Total Alkali-Silica; Le Maitre 2002) diagram and compositionally overlap with the majority of phonolites from the České středohoří Mts. (CS; Ackerman et al. 2015; Fig. 4). Most of the phonolites are metaaluminous to peralkaline with the values of the alkalinity index [molar $(K_2O+Na_2O)/Al_2O_3$] between 0.83 and 1.10. All samples have low Mg# [molar $100\times MgO/(MgO+FeO^{tot})$] ranging from 3 to 15, except for the phonolite from Sokol near Petrovice (sample NBPH3) yielding much higher Mg# of 69, most likely due to incorporation of some mantle-derived xenocrysts.

The major element contents of the phonolites from the Lužické hory Mts. display rather non-systematic correlations with SiO_2 contents. Overall, TiO_2 contents correlate positively, whereas Al_2O_3 and Na_2O are predominantly negatively correlated with increasing SiO_2 contents (with the exception of sample NBPH3 from Sokol near Petrovice with the lowest Na_2O content of 6.5 wt.% plotting outside of the correlation trend). The variation diagrams of selected major elements indicate partial compositional similarity of both phonolite types with those from the CS (Fig. 5).

Both types of phonolites, and especially type B phonolites, show elevated contents of incompatible elements such as Rb (A=161–255 ppm; B=229–474 ppm), U (A=5–13 ppm; B=10–24 ppm), Th (A=19–44 ppm; B=38–83 ppm), Zr (A=372–1023 ppm; B=1175–3037 ppm), Hf (A=10–16 ppm; B=20–57 ppm); Nb (A=131–207 ppm; B=110–937 ppm) and Ta (A=2–12 ppm; B=2–43 ppm). The presence of a linear

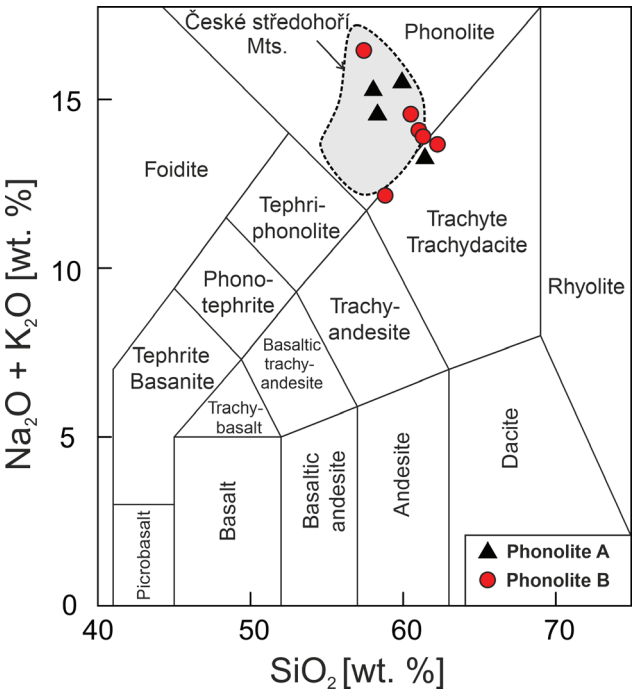

Fig. 4. Total alkali–silica (TAS) diagram (Le Maitre 2002) showing the composition of phonolite samples of the Lužické hory Mts. Shaded grey field represents composition of phonolitic rocks from the České středohoří Mts. (Ackerman et al. 2015).

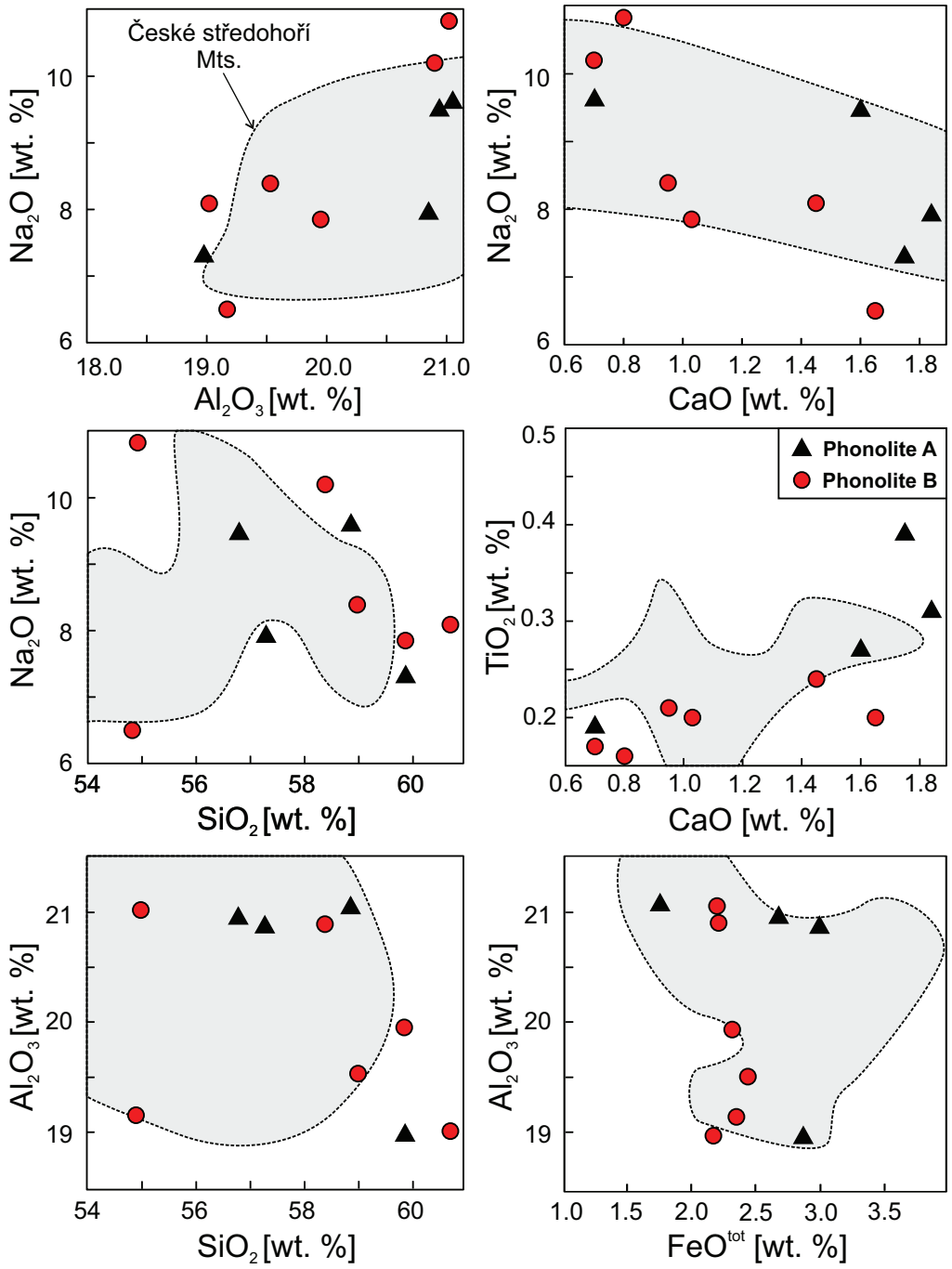

Fig. 5. Binary variation diagrams for selected major oxides in phonolites from the Lužické hory Mts. Shaded grey field represents variations in phonolitic rocks from the České středohoří Mts. (Ackerman et al. 2015).

trend between both phonolite types is clearly indicated in the trace element variation diagrams such as Zr *vs.* Rb or Th *vs.* U (Fig. 6), whereas non-linear trends are best displayed in Sr *vs.* Rb, Zr *vs.* Nb, U/Pb *vs.* Zr/Nb and Rb/Sr *vs.* Nb/Ta plots (Fig. 6). In both cases, phonolites of type A and B represent two end members of the differentiation series. The geochemical behaviour of major and trace elements during magmatic differentiation within the investigated phonolite types can be best seen in the normalized trace-element patterns (Fig. 7). The trace-element characteristics for most of the phonolites from the Lužické hory Mts. are similar to those described from the CS by Ackerman et al. (2015). Some of the investigated type B phonolites undergone higher degree of fractionation of feldspars, which is confirmed by higher variability of Al_2O_3 at relatively constant FeO^{tot} (Fig. 5) or by distribution of the primitive mantle normalized trace-element pattern with pronounced Ba and Sr troughs (Fig. 7).

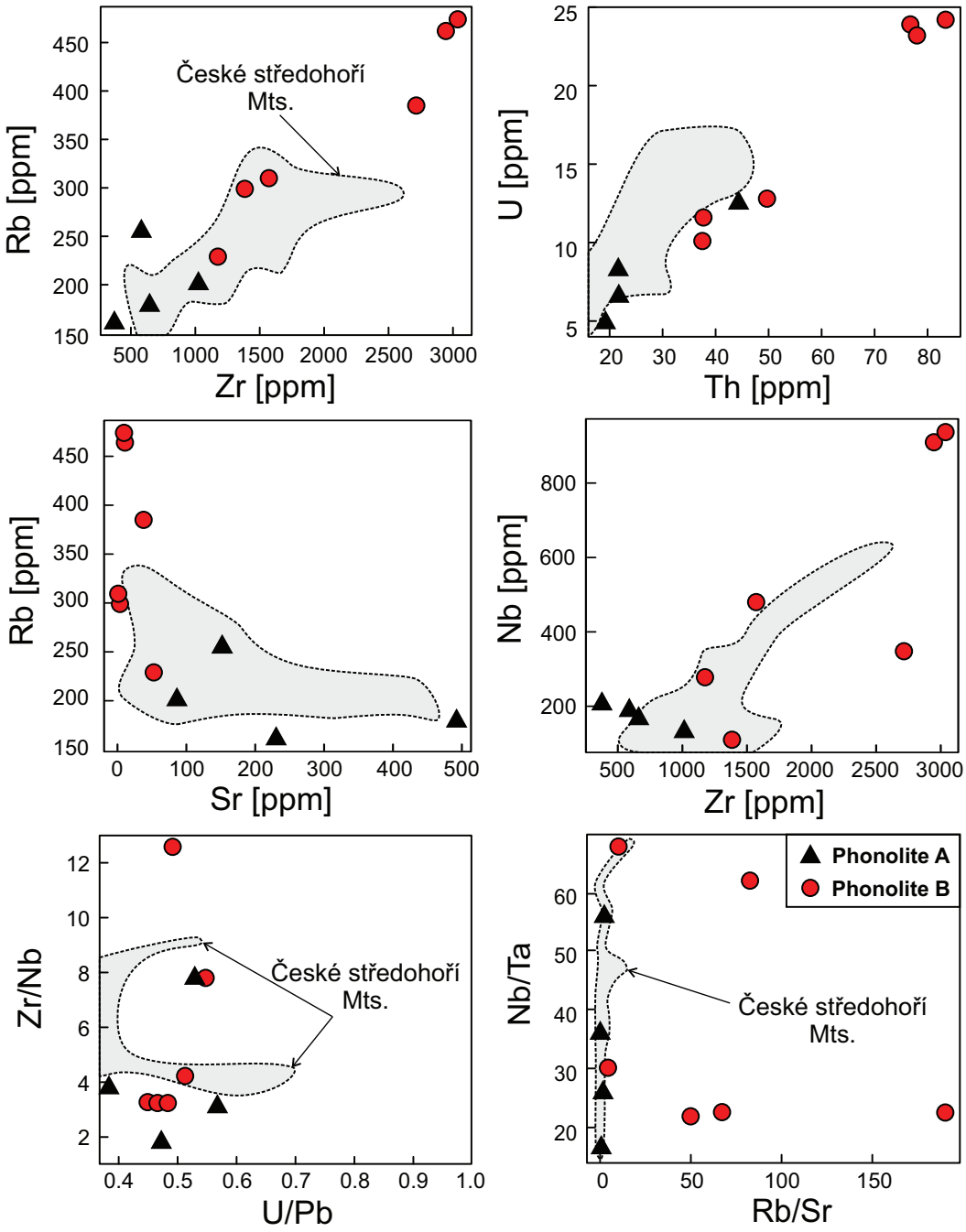

Fig. 6. Binary variation diagrams for selected trace elements and trace-element ratios of phonolites of the Lužické hory Mts. Shaded grey field represents variations in phonolitic rocks from the České středohoří Mts. (Ackerman et al. 2015).

Chondrite-normalized rare earth element (REE) patterns of the studied phonolites partly overlap, suggesting similar partial melting and fractional crystallization histories (Fig. 8). The samples show minor signs of U-shaped patterns with low abundances of the MREE. Negative Eu anomalies (Eu/Eu*= 0.4–0.6, higher Gd/Gd*=1.2–1.7 and lower La_N/Yb_N=10–29) are characteristic for B type of phonolites, while the A types of phonolites are characterized in the transitional values of Eu/Eu*=0.6–1.1, lower Gd/Gd*=0.28–1.6 and higher La_N/Yb_N =29–34 (Table 1). Compared to the CS samples, REE patterns of the studied phonolites are more scattered (Fig. 8). While the phonolite samples from Velký Buk and Sokol near Petrovice (type B) show the highest LREE enrichment, the sample from Luž (type B) displays a marked depletion of all REEs.

The CIPW normative calculation (Table 1) shows that all samples are nepheline-normative, confirming their silica-undersaturated, alkaline character. The norms are dominated by

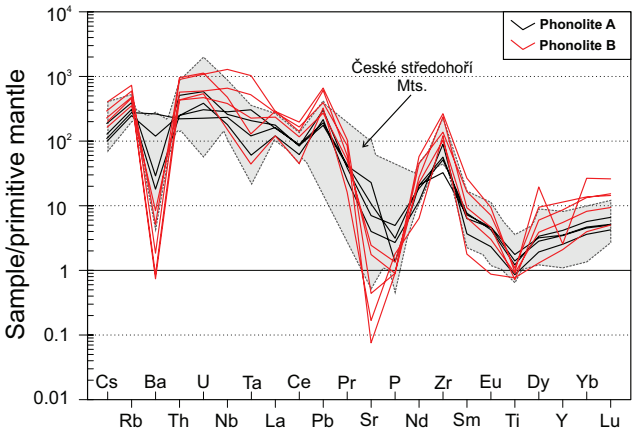

Fig. 7. Primitive mantle-normalized incompatible trace-element patterns for the phonolites from the Lužické hory Mts. Normalizing values are taken from McDonough & Sun (1995). Shaded grey field represents variations in phonolitic rocks from the České středohoří Mts. (Ackerman et al. 2015).

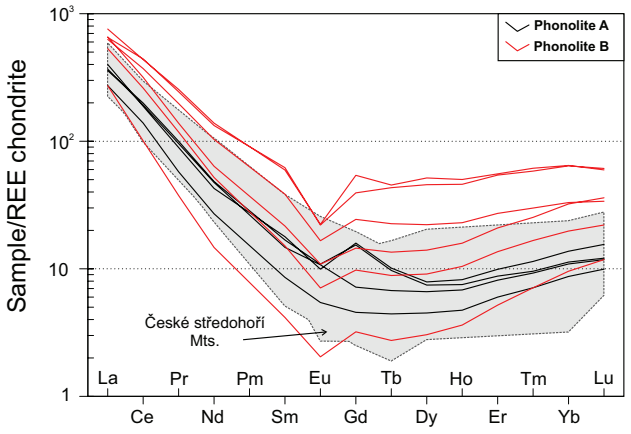

Fig. 8. Chondrite-normalized REE patterns of for the phonolites from the Lužické hory Mts. Normalization values were taken from Boynton (1984). Shaded grey field represents variations in phonolitic rocks from the České středohoří Mts. (Ackerman et al. 2015).

alkali feldspars (Or+Ab), accompanied by significant amounts of normative nepheline (up to ~28 %), consistent with a phonolitic composition. In several cases, normative acmite (aegirine) is also present, reflecting excess in Na_2O and Fe^{3+} typical of strongly alkaline phonolites.

K–Ar geochronology

Two phonolite whole-rock samples (both of type B) from the Lužické hory Mts. were analyzed for K–Ar ages (Table 2), yielding 34.2±1.4 and 26.7±1.1 Ma. Determined data correspond to the age of phonolites (~36–23 Ma; Ackerman et al. 2015) and the genetically associated basaltic rocks (36–21 Ma; Ulrych et al. 2002) from the CS, as well as to those from the other areas of the Lusatian Volcanic Field (~30 Ma; Büchner et al. 2024). However, we note that the ubiquitous excess of argon supposed to be preferentially concentrated in nepheline and/or sodalite (e.g., nepheline-rich and sodalite-poor phonolite from Sokol near Petrovice – 34 Ma) could largely account for the spread in the K–Ar ages (Balogh et al. 1999). Balogh in Ulrych et al. (2000b, 2005) and Pivec et al. (2004) assumed that a submicroscopic alteration associated with the change of the mineral structure may be responsible for the lowered Ar retention of nepheline and leucite and lower age.

Although this limited dataset cannot establish a firm geochronological framework, the results are presented here to provide additional context and to make the available data accessible, as no further K–Ar analyses could be carried out (performed by Kadosa Balogh†).

Sr–Nd–Pb isotope characteristics

The initial $^{87}Sr/^{86}Sr$ and $^{143}Nd/^{144}Nd$ data of phonolites from the Lužické hory Mts. define a linear horizontal array, generally showing a very large spread in Sr isotope ratios from ~0.6979 to 0.7142 contrasted by a relatively narrow range of ε_{Nd} values from +2.9 to +4.0 (Fig. 9; Table 3). In particular, the Sr-rich type A phonolites yielded relatively uniform initial $^{87}Sr/^{86}Sr$ of 0.7032–0.7039, with an exception of phonolite from Malý Stožec (sample 16PH4) with higher $^{87}Sr/^{86}Sr$ of 0.7098, while the most evolved, Sr-poor type B phonolites are characterized by contrastingly variable initial $^{87}Sr/^{86}Sr$ ratios, showing a decoupled horizontal trend on the Sr–Nd isotope diagram (Fig. 9). Such a large variation in Sr isotopes at fairly constant ε_{Nd} values documents that the Rb–Sr isotope system in these rocks was severely disturbed during late-stage processes modifying the Rb/Sr and $^{87}Sr/^{86}Sr$ ratios. Thus, the observed Sr isotope data of the type B phonolites are not sufficiently reliable for further interpretation of their

Table 2: K–Ar age data for phonolites from the Lužické hory Mts.

Sample	Rock type	Locality	Dated rock/mineral	K [%]	$^{40}Ar(rad)$ [cc STP/g]	$^{40}Ar(rad)$ [%]	Age±iσ [Ma]
16PH1	PH-B	Sokol, Petrovice	whole-rock	4.104	5.502×10^{-6}	66.8	34.2±1.4
NBPH1	PH-B	Velký Buk, Svor	whole-rock	4.080	4.866×10^{-6}	65.0	26.7±1.1

PH-B=type B phonolite.

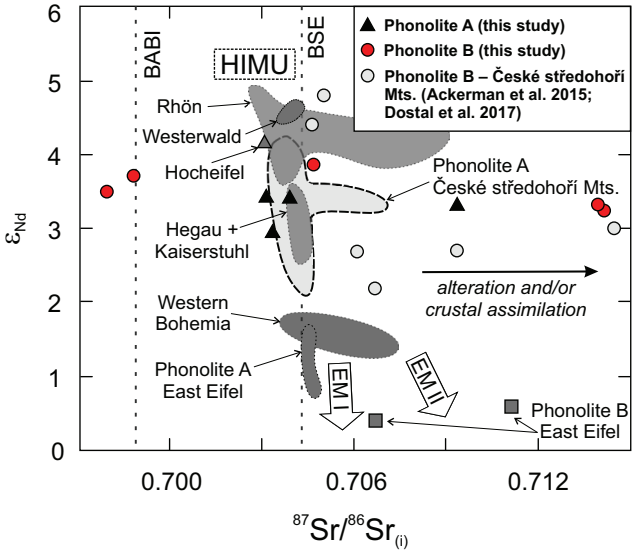

Fig. 9. Initial $^{87}Sr/^{86}Sr$ *vs.* ε_{Nd} isotope composition of phonolites from the Lužické hory Mts. Isotope data for phonolitic rocks of the České středohoří Mts. (Ackerman et al. 2015; Dostal et al. 2017), Western Bohemia (Ulrych et al. 2016), Rhön (Wedepohl et al. 1994; Jung et al. 2013; Mayer et al. 2013), Kaiserstuhl (Schleicher et al. 1991; Wedepohl et al. 1994), Hocheifel (Jung et al. 2006), East Eifel (Wörner et al. 1985; Wedepohl et al. 1994), Hegau and Westerwald (Wedepohl et al. 1994) are plotted for comparison. Sample NBPH1 has been exluded from this diagram due to its unreasonably low $^{87}Sr/^{86}Sr_{(i)}$ value (see Table 3). BSE=bulk silicate Earth; BABI=basaltic achondrite best initial; HIMU=high μ ($^{238}U/^{204}Pb$) unit; EM I=enriched mantle 1; EM II=enriched mantle 2 (Papanastassiou & Wasserburg 1969; Zindler & Hart 1986; Hart 1988).

origin as they clearly does not represent the magma source characteristics.

Initial lead isotope composition of both phonolite types falls within the following ranges: $^{206}Pb/^{204}Pb$=19.20–19.50, $^{207}Pb/^{204}Pb$=15.61–15.66 and $^{208}Pb/^{204}Pb$=39.07–39.30 (Fig. 10; Table 3). All samples form a nonlinear, rather scattered array with more distinct variation in $^{207}Pb/^{204}Pb$ isotope ratios in the $^{207}Pb/^{204}Pb$ *vs.* $^{206}Pb/^{204}Pb$ diagram. In contrast, the analyses show a nearly linear trend with only minor fluctuation of $^{208}Pb/^{204}Pb$ ratios at given $^{206}Pb/^{204}Pb$ values in the $^{208}Pb/^{204}Pb$ *vs.* $^{206}Pb/^{204}Pb$ diagram (Fig. 10).

Discussion

Information from major and trace-element composition

From the geochemical point of view, there is mostly overlap between the compositions of phonolites of type A and B, with an exception for stronger depletion in Ba and Sr, along with distinct enrichment in some incompatible elements (Fig. 7). In some plots (e.g., Fig. 5), the data do not clearly show two disticnt trends that can meaningfully separate both phonolite types. Based on the data presented, the most likely explanation is that the two phonolite groups represent end memebers of

Table 3: Sr–Nd–Pb isotope data for phonolites from the Lužické hory Mts.

No.	Sample	Rock type	Locality	Age [Ma]	$^{87}Sr/^{86}Sr_{(m)}$	$^{87}Sr/^{86}Sr_{(i)}$	$^{143}Nd/^{144}Nd_{(m)}$	$^{143}Nd/^{144}Nd_{(i)}$	ε_{Nd}	$^{206}Pb/^{204}Pb_{(m)}$	$^{207}Pb/^{204}Pb_{(m)}$	$^{208}Pb/^{204}Pb_{(m)}$	$^{206}Pb/^{204}Pb_{(i)}$	$^{207}Pb/^{204}Pb_{(i)}$	$^{208}Pb/^{204}Pb_{(i)}$
1	NBPH1	PH-B	Velký Buk, Svor	26.7	0.851897±10	*0.64021*	0.512784±6	0.51277	3.4	19.318	15.636	39.228	19.20	15.63	39.07
2	NBPH2	PH-B	Tolštejn, Jiřetín pod Jedlovou	30	0.726741±5	0.71419	0.512771±6	0.51276	3.2	19.531	15.646	39.490	19.36	15.64	39.30
3A	16PH1	PH-B	Sokol, Petrovice	34.2	0.775332±6	0.71246	0.512804±9	0.51279	3.9	19.501	15.671	39.411	19.33	15.66	39.23
3B	NBPH3	PH-B	Sokol, Petrovice	30	0.769222±7	0.70732	0.512776±5	0.51276	3.2	19.440	15.640	39.340	19.31	15.63	39.20
4	NBPH4	PH-A	Polevský vrch, Polevsko	30	0.704752±8	0.70389	0.512779±4	0.51277	3.4	19.484	15.642	39.314	19.34	15.64	39.16
5	NBPH5	PH-A	Klíč, Svor	30	0.706045±7	0.70317	0.512779±7	0.51277	3.4	19.501	15.652	39.423	19.34	15.64	39.28
6	16PH4	PH-A	Malý Stožec, Rybniště	30	0.709820±6	0.70937	0.512773±3	0.51276	3.3	19.614	15.670	39.444	19.50	15.66	39.29
7	NBPH7	PH-B	Luž, Mařenice	30	0.800696±9	*0.69791*	0.512781±9	0.51277	3.5	19.450	15.505	39.384	19.30	*15.50*	39.22
8	NBPH8	PH-A	Jedlová, Jiřetín pod Jedlovou	30	0.705468±6	0.70386	0.512758±6	0.51275	3.0	19.460	15.620	39.486	19.29	15.61	39.28
9	16PH5	PH-B	Sokol, Kytlice	30	0.704136±6	*0.69878*	0.512793±4	0.51278	3.7	19.580	15.639	39.448	19.42	15.63	39.26

PH-A = type A phonolite; PH-B = type B phonolite.
m = measured isotope ratio; i = initial isotope ratio.
Analytical uncertainties are given at $2\sigma_m$ level. Initial $^{87}Sr/^{86}Sr$ and ε_{Nd} were calculated using $\lambda^{87}Rb$ = 1.42E−11 y^{-1} and $\lambda^{147}Sm$= 6.54E−12 y^{-1}, $(^{147}Sm/^{144}Nd)^0_{CHUR}$ = 0.1960, and $(^{143}Nd/^{144}Nd)^0_{CHUR}$ = 0.512630 (Bouvier et al. 2008), respectively, and the concentration data given in Table 1.
Lead isotope data were recalculated using the constants recommended by IUGS ($\lambda^{232}Th$ = 4.9475E−11 y^{-1}, $\lambda^{235}U$ = 9.8485E−10 y^{-1}, $\lambda^{238}U$ = 1.55125E−10 y^{-1}), and the concentration data listed in Table 1.
Geologically unreasonably low recalculated values are given in italics.

a single mamga evolution (as documented also by presence of aegirine-component/Fe-poor or rich pyroxenes; Fig. 3), most probably reflecting rather different degree/material of crustal assimilation or late/post-magmatic metasomatism than two separate magma evolution trends.

High contents of incompatible elements, in particular Rb, U, Th, Zr, Hf, Nb and Ta are characteristic for highly alkaline phonolitic rocks that represent evolved products of the basanite–phonolite series (Le Roex et al. 1990; Jung et al. 2013; Ackerman et al. 2015). Low degrees (<5 %) of melting of a metasomatized mantle have given rise to primitive basanitic melts (Jung et al. 2013; Ackerman et al. 2015). Laporte et al. (2014) reported that such a low degree of partial melting of metasomatized lithospheric mantle at 1.0–1.5 GPa can also produce rocks of phonolitic compositions, but such melts would have Mg# values around 70. Since the Lužické hory Mts. phonolites yielded much lower Mg# values (3–15), except for one sample from Sokol near Petrovice (NBPH3) with Mg#=69 reflecting presence of mantle xenoliths, their origin as direct mantle melts can be ruled out, and evolution by fractional crystallization of parental basanites seems to be the best explanation (Choi 2021).

The distribution coefficients ($D^{mineral/melt}$) for selected incompatible elements (e.g., Zr, Y, La) generally increase with degree of alkalinity and differentiation of the magma. This trend has been confirmed in the case of Zr in the Tristan da Cunha lavas by Le Roex et al. (1990) analysing clinopyroxene phenocrysts for Zr and comparing to the concentration data with the bulk rock analyses. Approximate distribution coefficients range from 0.5 in basanite to 1.2 in phonolite (Le Roex et al. 1990). Zirconium in studied phonolites is concentrated in rims of aegirine-augite phenocrysts (ZrO_2=0.5–0.7 wt.%; Supplementary Material S1C), and up to 1.2 wt.% in aegirine rims and acicular needles in the groundmass (Kühn 1990). High Zr concentrations are associated to the late-magmatic to post-magmatic mineral phases such as hainite, fluorian eudialyte and vlasovite in vesicles and veinlets (Kühn 1990; Supplementary Material S1D). Hibsch (1934) originally described two types of hainite – needle-shaped crystals of hainite I occuring in miarolitic cavities and rarely also in the groundmass (up to 1 mm), and thin lobate lamellae of hainite II exclusively bound to the groundmass. Kühn (1990), Ulrych et al. (1992) and Skála et al. (2010) later specified their chemical compositions, hovewer, the reported empirical formulae of both types differed considerably, which does not allow a clear classification of both types based on their chemical composition. Additionally, Kühn (1990) reported also the third type of hainite having increased content of Ti, Zr, Mn, Fe, Nb and Al at the expense of alkalis, especially Ca, being probably an alteration product of other Zr-bearing phases. Considering the tabular appearance of hainite in the groundmass (up to 0.02 mm) of studied samples as well as its chemical composition close to that published by Skála et al. (2010) for hainite II (except for Y, Nb, Ta and REE that were not determined in studied samples; see Supplementary Material S1D), we classified the observed minerals as hainite II.

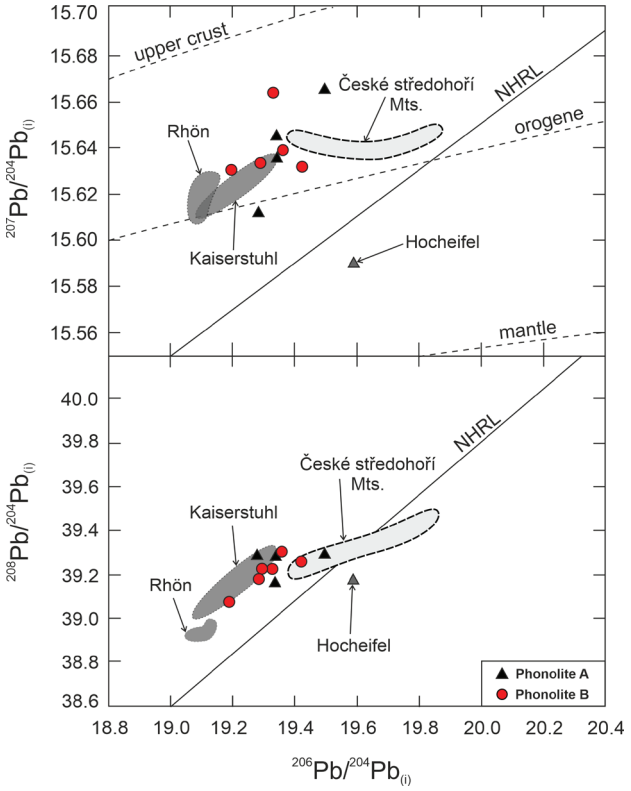

Fig. 10. Initial Pb isotope composition of phonolites from the Lužické hory Mts. Isotope data for phonolitic rocks of the České středohoří Mts. (Krmíčková et al. 2020), Rhön (Jung et al. 2013; Mayer et al. 2013), Kaiserstuhl (Schleicher et al. 1991) and Hocheifel (Jung et al. 2006) are plotted for comparison. Upper crust, orogenic and mantle growth curves are adopted from Zartman & Doe (1981). NHRL=northern hemisphere reference line (Hart 1984).

The primitive mantle-normalized incompatible trace-element patterns of the studied rocks exhibit a number of characteristic features (Fig. 7). For example, pronounced negative Sr, Ba (Sr<20 ppm, Ba<60 ppm) and Eu (Fig. 8) anomalies in type B phonolites are clearly associated with preceding feldspar crystallization and, therefore, should be related to the formation of phonolites as evolved, low-pressure fractional crystallization products of basanitic magma (Wilson et al. 1995; Ackerman et al. 2015). At the same time, negative P and Ti anomalies support the important role of apatite, Ti-magnetite or alternatively amphibole fractionation during the melt evolution. On the other hand, the higher Ba and Sr contents (Sr>90 ppm, Ba>130 ppm) in type A phonolites correspond to lower extent of clinopyroxene and especially feldspar crystallization from parental basanitic magma (as documented by Al_2O_3/FeO^{tot} diagram in Fig. 5), similar to that already ascribed to phonolites from the nearby České středohoří Mts. (CS; Ackerman et al. 2015). The omnipresent positive Zr (and Hf) and rare positive Nb (and Ta) anomalies might indicate OIB-like reworked subducted Variscan material genetically related to the European asthenospheric reservoir (EAR *sensu* Granet et al. 1995 and Wilson & Bianchini 1999) or the common mantle reservoir (CMR) characteristic for Cenozoic

intra-plate volcanism in Europe (Lustrino & Wilson 2007). Ulrych & Pivec (1997) also noted that crustal contamination by a specific Zr-rich material, e.g., by sediments of the Bohemian Cretaceous Basin with medium (150–200 ppm) up to very high (about 20,000 ppm) Zr contents and the variable Nb concentrations (50–250 ppm) should be also considered as a plausible scenario. However, the most likely explanation for the observed phonolite enrichment in HFSE such as Zr, Nb, Hf, Ta, U, Th, together with elevated Zr/Nb in low-Sr type B phonolites is due to the enrichment in these elements in the late-magmatic to post-magmatic fluids that were derived from Zr-rich Cretaceous sedimentary rocks, in which the phonolites intruded. Such an enrichment of the surrounding sedimentary rocks in Zr, REE, U and other elements may originate from ultramafic lamprophyres (polzenites; 80 Ma) that are abundant in the northern Bohemia region, as documented also by presence of infiltration uranium deposits situated along the Stáž Fault (Ulrych et al. 1992, 2014, 2022; Skála et al. 2015; Krmíčková et al. 2020; Mikysek et al. 2021). Nevertheless, the AFC modelling of basanite–phonolite crystallization from the CS (Ackerman et al. 2015) has shown that Zr/Nb ratios strongly increase as a consequence of the segregation of amphibole and plagioclase during progressive melt evolution.

A remarkably high Zr contents may be also connected to the high solubility of alkali zirconium silicate complexes in strongly alkaline melts, where they can form fluorine-complexes such as $(ZrF_6)^{2-}$, $(NbF_7)^{2-}$ in the presence of high fluorine contents (Watson 1979; Ulrych et al. 1992). Higher fluorine concentrations in the phonolite magmas may have also a favourable influence on the transport of Zr in weakly acidic solutions. In such a highly alkaline environment, Zr and Nb behave as anions as they are amphoteric elements in nature. Wilson et al. (1995) suggested that observed U-shaped chondrite-normalized REE patterns with low abundances of the MREE may have been caused by the fractionation of amphibole and/or titanite (Fig. 8). As noted by Ackerman et al. (2015), the overall high enrichment of incompatible elements in phonolites can be best explained by segregation of amphibole and plagioclase during progressive melt evolution followed by the late-magmatic to post-magmatic crystallization of Zr-rich minerals in miarolitic cavities.

We suggest that tectonic zones of the Lusatian Fault and Stráž Fault served as a feeding channel of the hydrothermal fluids with incompatible elements including Zr and other trace elements. The model of Kühn (1990) shows that the distribution of REE, Y and Nb in phonolitic bodies of the Lužické hory Mts. is primarily controlled with the NE–SW directions (Stráž Fault) corresponding to the Ohře (Eger) Rift structure, while the distribution of Zr, U, Th and Rb is mostly controlled with the NW–SE trending Lusatian Fault, representing the major structure of the area.

Information from Sr–Nd–Pb isotopes

Radiogenic isotope composition such as Sr–Nd–Pb represent a reliable tool to characterize the source of mantle-derived rocks. However, in case of highly differentiated volcanic rocks such as phonolites, it is important to evaluate whether their source has been modified by assimilation of material with a different isotope composition during the magma evolution. As the pristine upper mantle source is generally characterized by low Pb contents compared to primitive mantle (e.g., Sun 1982; Salters et al. 2002; Hart & Gaetani 2006; Panter et al. 2006), the isotope composition of the mantle and mantle-derived rocks has been readily affected during metasomatism (Brenan et al. 1995; Keppler 1996; Krmíčková et al. 2020). Due to the contrasting Pb contents in the crust and mantle, however, even small contributions of continental material are more sensitively recorded by Pb isotopes than in Sr–Nd isotope composition (e.g., Sun & McDonough 1989; Panter et al. 1997; Jung et al. 2013; Wiesmaier et al. 2013; Krmíčková et al. 2020; Pontesilli et al. 2022). Whereas the Sr–Nd isotope compositions of phonolitic rocks from the Bohemian Massif were investigated in several studies (Ackerman et al. 2015; Ulrych et al. 2016; Dostal et al. 2017), the Pb isotope data are rather limited (Krmíčková et al. 2020).

The Sr–Nd isotope composition of phonolites from the Lužické hory Mts. indicates their origin from moderately depleted mantle sources similar to common Cenozoic volcanic rocks from Europe known as a sub-lithospheric common mantle reservoir (CMR) defined by Lustrino & Wilson (2007). Yet, it appears that the parental mantle-derived magma of the studied phonolites is characterized by less radiogenic Nd and partly by more radiogenic Sr than those found in common Cenozoic mafic rocks of the Bohemian Massif (Ulrych & Pivec 1997). The wide range of $^{87}Sr/^{86}Sr$ ratios at roughly constant ε_{Nd} (Fig. 9), which is more pronounced in the type B phonolites, cannot reflect such large variations in mantle source compositions, and can be attributed to (i) undercorrection of initial $^{87}Sr/^{86}Sr$ ratios in the higher $^{87}Sr/^{86}Sr$ samples due to post-emplacement alteration, to (ii) increased present-day $^{87}Sr/^{86}Sr$ ratios through late-stage interaction with high $^{87}Sr/^{86}Sr$ hydrothermal fluids or (iii) extensive fractionation of plagioclase. Overall, such perturbation(s) even resulted in initial $^{87}Sr/^{86}Sr$ values of ~0.698 that are below the BABI (basaltic achondrite best initial) ratio (cf. Papanastassiou & Wasserburg 1969). Largely homogeneous ε_{Nd} values suggest that an extensive crustal contamination was unlikely involved in the formation of these felsic magmas. Still, some minor assimilation of crustal material (most probably of the Bohemian Cretaceous Basin sedimentary rocks with elevated Zr contents; cf. Ulrych & Pivec 1997) cannot be completely ruled out, as the very low Sr but high Nd concentrations detected in phonolites (Table 1) would result in significantly modified Sr but not Nd isotope compositions (Choi 2021).

Wedepohl et al. (1994) suggested that the higher Sr isotope values >0.706 detected in type B phonolites reflect a modification by granitic partial melts from the wall rock of the magma chamber. Similar trends of low-Sr phonolite Sr–Nd isotope characteristics are presented also from the Laacher See Quarternary phonolite volcano in East Eifel (Wörner et al. 1985), central Scotland (Upton et al. 2007) or Ulleung Island

in South Korea (Choi 2021). Wörner et al. (1985) documented an inverse relationship between Sr concentrations and $^{87}Sr/^{86}Sr$ ratios, but this can only be applied to very young volcanic rocks, as their initial isotope composition is not significantly modified due to radiogenic *in situ* growth over time. No similar correlation was observed in initial Sr isotope compositions of our samples, but can be noticed in their measured $^{87}Sr/^{86}Sr$ values (Table 3). However, generally high $^{87}Sr/^{86}Sr$ ratios of the type B phonolite reflect depletion of Sr, resulting in high Rb/Sr ratios, which play a significant role in recalculation to initial Sr isotope values (Choi 2021). Moreover, a caution is needed when comparing with our case, as the Laacher See magma chamber and erupted volumes were much larger, and potential assimilation effects may scale differently in smaller systems.

Similar behaviour of Sr–Nd isotope systematics was observed also in phonolites of the České středohoří Mts. (CS; Ackerman et al. 2015; Dostal et al. 2017), Western Bohemia (Ulrych et al. 2016) and Rhön (Wedepohl et al. 1994; Jung et al. 2013; Mayer et al. 2013). The type A phonolites from the Lužické hory Mts. best correspond to the type A phonolites from the CS, having only slightly higher range of the $^{87}Sr/^{86}Sr$ ratios at the same ε_{Nd} values. The Rhön Cenozoic phonolites are characterized also by the large range of $^{87}Sr/^{86}Sr$ (0.70332–0.70884) at relatively narrow range but higher values of ε_{Nd} (+3.7 to +4.8; Wedepohl et al. 1994; Jung et al. 2013; Mayer et al. 2013). The EM I trend reflecting an enrichment of the mantle source by recycled lower crust or mantle metasomatism by deep CO_2-rich fluids (Menzies 1983; Zindler & Hart 1986), which is prominent in several type A phonolites from the CS (Ackerman et al. 2015; Dostal et al. 2017), Rhön (Wedepohl et al. 1994; Jung et al. 2013; Mayer et al. 2013), Hegau, Kaiserstuhl or East Eifel (Wedepohl et al. 1994), does not occur in the phonolites from the Lužické hory Mts. in general (Fig. 9). Crustal assimilation is hardly detectable in high-Sr phonolites of type A (Sr >100 ppm) from Rhön (Jung et al. 2013), but may be recognized by subtle variations in Nd and Pb isotope compositions in contrast to low-Sr phonolites of type B (Sr <100 ppm; Wedepohl et al. 1994). The initial Sr–Nd isotope signature of low-Sr phonolites from the Lužické hory Mts. area correspond mainly to phonolites of type B (*sensu* Ackerman et al. 2015) from the CS, showing the same significant increase of $^{87}Sr/^{86}Sr$ at given ε_{Nd} towards more differentiated compositions (cf. Wörner et al. 1985).

The phonolites from the Lužické hory Mts. evolved from parental amphibole-bearing basanites, having slightly less radiogenic initial $^{87}Sr/^{86}Sr$ values of ~0.7035 (Haase & Renno 2008), along a differentiation trend that is controlled by the separation of a series of mafic and felsic minerals. Magmas have experienced variable degrees of crystal fractionation and limited mixing in conduits *en route* to the surface (over a depth range of 1.4 to 8 kbar; Le Roex et al. 1990). The phonolites seem to have evolved by (i) pure fractional crystallization, indicated, e.g., by increasing incompatible trace element concentrations at virtually constant ε_{Nd} values of +2.9 to +3.4 and $^{87}Sr/^{86}Sr$ ratios of 0.7032 to 0.7094 (type A) or by (ii) a process, which involved assimilation-fractional crystallization process (AFC) producing evolved magmas characterized by partly higher range of ε_{Nd} (+3.2 to +3.8) and broad range of $^{87}Sr/^{86}Sr$ up to 0.7142 (type B). Already published data for phonolitic rocks (Le Roex et al. 1990; Ackerman et al. 2015) show also substantial variation of $^{87}Sr/^{86}Sr$ and ε_{Nd} in type B and lesser in type A. These features may result from assimilation of various amount of crustal material by differentiating parental magma rather than from mantle source enrichment (Wörner et al. 1985, 1986). This is in accordance with observations of Wedepohl et al. (1994) and Wörner et al. (1985) who indicated that low-Sr phonolites (type B) with Sr <100 ppm are more prone to show effects of crustal contamination due to the strong contrast in Sr concentrations and isotope compositions between these phonolites and lower and/or upper crustal country rocks.

Character of the mantle source of the phonolites can be much more sensitively recorded by Pb isotopes than by Sr isotopes as the disturbance of the Rb–Sr systematics as post-magmatic processes typically does not affect the initial Pb isotope signatures (e.g., Halliday et al. 1988; Schleicher et al. 1990; Jiang 2005; Jung et al. 2013). Lead isotope composition of the phonolites from the Lužické hory Mts. plots along the orogenic growth curve with a slight inclination towards the upper crust growth curve of Zartman & Doe (1981) in the $^{206}Pb/^{204}Pb$ *vs.* $^{207}Pb/^{204}Pb$ diagram, and fall above the northern hemisphere reference line (NHRL) of Hart (1984) in the $^{206}Pb/^{204}Pb$ *vs.* $^{208}Pb/^{204}Pb$ diagram (Fig. 10). A linear mixing trend typical for majority of alkaline lavas from the Central European Volcanic Province (Krmíčková et al. 2020 and references therein), including evolved phonolitic rocks from the České středohoří Mts. (CS; Krmíčková et al. 2020) or Kaiserstuhl (Schleicher et al. 1991), is not prominent in the investigated phonolites in the $^{206}Pb/^{204}Pb$ *vs.* $^{207}Pb/^{204}Pb$ diagram as some of their $^{207}Pb/^{204}Pb$ ratios are shifted to higher values at given $^{206}Pb/^{204}Pb$ (Fig. 10) due to various degree of assimilation-fractional crystallization (AFC) of the differentiated lavas (Haase et al. 2004; Jung et al. 2012; Kolb et al. 2012). Similar effect of the AFC process on the $^{207}Pb/^{204}Pb$ ratios has been reported for phonolites from the Rhön area having larger range of $^{207}Pb/^{204}Pb$ values at low and narrow $^{206}Pb/^{204}Pb$, reflecting an involvement of older lower crustal material in their primarily mantle-derived parental magma (Jung et al. 2013; Mayer et al. 2013). Another factor that supports possible assimilation of U/Pb-poor lower continental crust is that phonolites from the Lužické hory Mts. have less radiogenic $^{206}Pb/^{204}Pb$ ratios compared to their parental basanitic rocks (Haase & Renno 2008; Rudnick & Gao 2014; Choi 2021). Different Pb isotope composition characterized by radiogenic $^{206}Pb/^{204}Pb$ and unradiogenic $^{207}Pb/^{204}Pb$ and $^{208}Pb/^{204}Pb$ ratios, plotting distinctively below the orogenic growth curve and NHRL, respectively, has been documented for phonolite from the Hocheifel area (Jung et al. 2006). These rocks were derived from the asthenospheric mantle during the initial stage of continental rifting in the Rhine Graben area, similarly as in case of the Ohře (Eger) Rift, where the initial syn-rift lavas show resembling isotope trends (Blusztajn &

Hart 1989; Krmíčková et al. 2020). Considering the determined ages of the phonolites from the Lužické hory Mts. between 34 and 27 Ma, these rocks formed much later after the initial phase of the syn-rift period around 42 Ma (Ulrych & Pivec 1997; Ulrych et al. 2011). Thus, their isotope composition is shifted to less radiogenic $^{206}Pb/^{204}Pb$ lying above the NHRL (Fig. 10), indicating a greater contribution of the asthenospheric-derived melts to their metasomatically enriched lithospheric mantle source as the rifting proceeded (Krmíčková et al. 2020), similarly as in case of other volcanic rocks from the Lužické hory Mts. (Haase & Renno 2008). In contrast to the Sr–Nd isotopes, substantial difference between A-type and B-type phonolites from the Lužické hory Mts. has not been recorded by the Pb isotopes, suggesting that they were derived from the same mantle source and their composition was diversified later during the post-magmatic processes.

Conclusions

The phonolites of the Lusatian Fault area are the most evolved members of the strongly alkaline basanite/tephrite–phonolite series of the Lužické hory Mts. emplaced between ~34 to 27 Ma. Based on the observed petrography, crystallization of the phonolites proceeded primarily in three stages: (i) early magmatic stage represented by rare (micro)phenocrysts of alkali feldspars (anorthoclase to sanidine), feldspathoids (nepheline, sodalite), pyroxene and amphibole, (ii) main magmatic stage dominated by groundmass consisting of felsic minerals (anorthoclase, sanidine, plagioclases, sodalite) and (aegirine)augite, and (iii) late-magmatic to post-magmatic stage associated with the formation of hydrous minerals such as analcime, and activity of residual fluids rich in Zr–Nb–REE–Ti (concentrated in hainite, Nb-rich titanite and aegirine rims).

Two geochemically different phonolite types were recognized. Phonolites of type A (high Sr and Ba) are characterized by initial $^{87}Sr/^{86}Sr$ from ~0.7032 to 0.7094 and ε_{Nd} values from +2.9 to +3.4. On the other hand, the type B phonolites (low Sr and Ba) show markedly decoupled Sr–Nd signatures ($^{87}Sr/^{86}Sr$ = ~0.6979 to 0.7142 at ε_{Nd} values from +3.2 to +3.8), reflecting a strong post-emplacement disturbance of Sr isotope systematics, while Pb isotope composition of both types overlaps. Highly differentiated B-type phonolitic magma may be modified by assimilation of lower continental crust during their evolution, as evidenced by higher $^{87}Sr/^{86}Sr$ ratios at given ε_{Nd}, and highly radiogenic $^{207}Pb/^{204}Pb$ ratios at given less radiogenic $^{206}Pb/^{204}Pb$. Both phonolite types originated through the assimilation-fractional crystallization of parental mafic melts derived by low-degree melting of a sub-lithospheric source with either OIB-like or common mantle reservoir (CMR) character (Lustrino & Wilson 2007). The primary basanitic melts undergone significant fractionation crystallization connected with crustal assimilation (e.g., Ulrych et al. 2011; Ackerman et al. 2015). The principal role in the geochemical characteristic of most of the phonolites from the Lužické hory Mts. in terms of selected incompatible elements as Rb, REE, Zr, Hf, U, Th, Nb and Ta can be best explained by high degree of fractionation; in case of type B phonolites also in combination with percolation of late-stage magmatic to post-magmatic fluids rich in F and Cl. The percolation of these fluids in the studied area is associated with fault systems present within the Lusatian Fault Zone. Phonolites of type A and B are therefore best understood as two end memebers of a single mamgatic evolution, distinguished by the extent and character of crustal assimilation or by different degree of late/post-magmatic overprinting, rather than as products of two independent magmatic evolutionary trends.

Acknowledgements: The manuscript was benefitted from the comments of Jaroslav Dostal, Saint Mary's University, Halifax, Nova Scotia, and Felicity E. Lloyd, University of Bristol. Thanks are also given to Zuzana Korbelová, Jiří Karel Novák, Miloš Lang and Roman Skála for help with microprobe analyses, Jana Rajlichová for technical assistance, and Jan Rejšek for TIMS measurements, all from the Institute of Geology, Czech Academy of Sciences, Prague. The authors greatly appreciate Tamás Sági and an anonymous reviewer for very constructive review, helpful comments and suggestions, and Silvia Antolíková and Igor Broska for the editorial work. This research was financially supported by the institutional project of the Institute of Geology of the Czech Academy of Sciences (grant number RVO 67985831)]. K–Ar dating, carried out by Kadosa Balogh†, Institute of Nuclear Sciences, Debrecen, was covered by OTKA projects (grant numbers T060965, M41434).

References

Ackerman L., Ulrych J., Řanda Z., Erban V., Hegner E., Magna T., Balogh K., Frána J., Lang M. & Novák J.K. 2015: Geochemical characteristics and petrogenesis of phonolites and trachytic rocks of the České Středohoří Volcanic Complex, the Ohře Rift, Bohemian Massif. *Lithos* 224–225, 256–271. https://doi.org/10.1016/j.lithos.2015.03.014

Ackerman L., Žák K., Skála R., Rejšek J., Křížová Š., Wimpenny J. & Magna T. 2020: Sr–Nd–Pb isotope systematics of Australasian tektites: Implications for the nature and composition of target materials and possible volatile loss of Pb. *Geochimica Cosmochimica Acta* 276, 135–150. https://doi.org/10.1016/j.gca.2020.02.025

Balogh K. 1985: K/Ar dating of Neogene volcanic activity in Hungary: Experimental technique, experience and methods of chronological studies. *ATOMKI Közlemények* 27, 277–288.

Balogh K., Ahijado A., Casillas R. & Fernandez C. 1999: Contributions to the chronology of the Basal Complex of Fuerteventura, Canary Islands. *Journal of Volcanology and Geothermal Research* 30, 81–101. https://doi.org/10.1016/S0377-0273(99)00008-6

Bernth U., Brousse R., Frei R. & Sørensen H. 2002: The Origin of phonolites and trachytes from the Col de Guéry area: Le Mont-Dore, Massif Central, France. *Matematisk-fysiske Meddelelser* 50, 1–61.

Binder T., Marks M. A., Friedrichsen B. E., Walter B. F., Wenzel T. & Markl G. 2024: Bimodal volcanism in the Hegau region (SW Germany): differentiation of primitive melilititic to nephelinitic rocks produces evolved nosean phonolites. *Lithos* 472, 107565. https://doi.org/10.1016/j.lithos.2024.107565

Binder T., Marks M. A., Gerdes A., Walter B. F., Grimmer J., Beranoaguirre A., Wenzel T. & Markl G. 2023: Two distinct age groups of melilitites, foidites, and basanites from the southern Central European Volcanic Province reflect lithospheric heterogeneity. *International Journal of Earth Sciences* 112, 881–905. https://doi.org/10.1007/s00531-022-02278-y

Blumrich J. 1883: Die Phonolite des Friedländer Bezirkes in Nordböhmen. *Tschermaks Mineralogische und Petrographische Mitteilungen* 13, 465–595. https://doi.org/10.1007/BF03000116

Blusztajn J. & Hart S.R. 1989: Sr, Nd, and Pb isotopic character of Tertiary basalts from southwest Poland. *Geochimica Cosmochimica Acta* 53, 2689–2696. https://doi.org/10.1016/0016-7037(89)90140-3

Bouvier A., Vervoort J.D. & Patchett P.J. 2008: The Lu–Hf and Sm–Nd isotopic composition of CHUR: constraints from unequilibrated chondrites and implications for the bulk composition of terrestrial planets. *Earth and Planetary Science Letters* 273, 48–57. https://doi.org/10.1016/j.epsl.2008.06.010

Boynton W.V. 1984: Cosmochemistry of the rare earth elements: meteorite studies. *Developments in Geochemistry* 2, 63–114. https://doi.org/10.1016/B978-0-444-42148-7.50008-3

Brenan J.M., Shaw H.F., Ryerson F.J. & Phinney D.L. 1995: Mineral-aqueous fluid partitioning of trace elements at 900 °C and 2.0 GPa: Constraints on the trace element chemistry of mantle and deep crustal fluids. *Geochimica et Cosmochimica Acta* 59, 3331–3350. https://doi.org/10.1016/0016-7037(95)00215-L

Briot D., Cantagrel J.M., Dupuy C. & Harmon R.S. 1991: Geochemical evolution in crustal magma reservoirs: trace-element and Sr–Nd–O isotopic variations in two continental intraplate series at Monts Dore, Massif Central, France. *Chemical Geology* 89, 281–303. https://doi.org/10.1016/0009-2541(91)90021-I

Büchner J., Tietz O., Viereck L., Suhr P. & Abratis M. 2015: Volcanology, geochemistry and age of the Lausitz Volcanic Field. *International Journal of Earth Sciences* 104, 2057–2083. https://doi.org/10.1007/s00531-015-1165-3

Büchner J., Gerdes A., Viereck L., Tietz O. & Seifert W. 2024: Zircon megacrysts in alkaline lavas of the Lusatian Volcanic field (Central Europe)-petrogenetic implications of U/Pb ages, Hf isotopes and trace element characteristics. *Journal of Applied & Regional Geology* 175, 11–34. https://doi.org/10.1127/zdgg/2023/0408

Choi S.H. 2021: Geochemistry and petrogenesis of Quaternary volcanic rocks from Ulleung Island, South Korea. *Lithos* 380, 105874. https://doi.org/10.1016/j.lithos.2020.105874

Coubal M., Adamovič J., Málek J. & Prouza V. 2014: Architecture of thrust faults with along strike variations in fault-plane dip: anatomy of the Lusatian Fault, Bohemian Massif. *Journal of Geosciences* 59, 183–208. https://doi.org/10.3190/jgeosci.174

Dèzes P., Schmid S.M. & Ziegler P.A. 2004: Evolution of the European Cenozoic Rift System: interaction of the Alpine and Pyrenean orogens with their foreland lithosphere. *Tectonophysics* 389, 1–33. https://doi.org/10.1016/j.tecto.2004.06.011

Dollase W.A. & Thomas W.M. 1978: The crystal chemistry of silica-rich, alkali-deficient nephelines. *Contributions to Mineralogy and Petrology* 66, 311–318. https://doi.org/10.1007/BF00373415

Dostal J., Shellnutt J.G. & Ulrych J. 2017: Petrogenesis of the Cenozoic alkaline volcanic rock series of the České Středohoří Complex (Bohemian Massif), Czech Republic: A case for two lineages. *American Journal of Science* 317, 677–706. https://doi.org/10.2475/06.2017.02

Granet M., Wilson M. & Achauer U. 1995: Imaging mantle plumes beneath the French Massif Central. *Earth and Planetary Science Letters* 136, 199–203. https://doi.org/10.1016/0012-821X(95)00174-B

Haase K.M. & Renno A.D. 2008: Variation of magma generation and mantle sources during continental rifting observed in Cenozoic lavas from the Eger Rift, Central Europe. *Chemical Geology* 257, 192–202. https://doi.org/10.1016/j.chemgeo.2008.09.003

Haase K.M., Goldschmidt B. & Garbe-Schönberg C.D. 2004: Petrogenesis of Tertiary continental intra-plate lavas from the Westerwald region, Germany. *Journal of Petrology* 45, 883–905. https://doi.org/10.1093/petrology/egg115

Halliday A.N., Dickin A.P., Fallick A.E. & Fitton J.G. 1988: Mantle dynamics: a Nd, Sr, Pb and O isotopic study of the Cameroon line volcanic chain. *Journal of Petrology* 29, 181–211. https://doi.org/10.1093/petrology/29.1.181

Harangi S. 1994: Geochemistry and petrogenesis of the Early Cretaceous continental rift-type volcanic rocks of the Mecsek Mountains, South Hungary. *Lithos* 33, 303–321. https://doi.org/10.1016/0024-4937(94)90035-3

Harangi S. & Lenkey L. 2007: Genesis of the Neogene to Quaternary volcanism in the Carpathian-Pannonian region: Role of subduction, extension, and mantle plume. *Geological Society of America Special Papers* 418, 67–92. https://doi.org/10.1130/2007.2418(04)

Harangi S., Seghedi I. & Lukács R. 2026: The Neogene–Quaternary volcanism of the Carpathian–Pannonian region: from initial plate tectonic models to quantitative petrogenetic explanations. *Geological Society, London, Special Publications* 554, SP554-2024-84. https://doi.org/10.1144/SP554-2024-84

Hart S.R. 1984: A large-scale isotope anomaly in the Southern Hemisphere mantle. *Nature* 309, 753–757. https://doi.org/10.1038/309753a0

Hart S.R. 1988: Heterogeneous mantle domains: signatures, genesis and mixing chronologies. *Earth and Planetary Science Letters* 90, 273–296. https://doi.org/10.1016/0012-821X(88)90131-8

Hart S.R. & Gaetani G.A. 2006: Mantle Pb paradoxes: the sulfide solution. *Contributions to Mineralogy and Petrology* 152, 295–308. https://doi.org/10.1007/s00410-006-0108-1

Hibsch J.E. 1930: Geologischer Führer durch das Böhmische Mittelgebirge. *Gebrüder Bornträger*, Berlin, 1–384. https://doi.org/10.23689/fidgeo-3305

Hutchison C.S. 1974: Laboratory Handbook of Petrographic Techniques. *John Wiley & Sons*, New York, 1–527.

Hutchison C.S. 1975: The norm, its variations, their calculation and relationships. *Schweizerische mineralogische und petrographische Mitteilungen* 55, 243–256.

Jiang N. 2005: Petrology and geochemistry of the Shuiquangou syenitic complex, northern margin of the North China Craton. *Journal of the Geological Society* 162, 203–215. https://doi.org/10.1144/0016-764903-144

Jochum K.P. & Nohl U. 2008: Reference materials in geochemistry and environmental research and the GeoReM database. *Chemical Geology* 253, 50–53. https://doi.org/10.1016/j.chemgeo.2008.04.002

Johnson W.M. & Maxwell J.A. 1981: Rock and Mineral Analysis. *Wiley*, New York, 1–489.

Jung C., Jung S., Hoffer E. & Berndt J. 2006: Petrogenesis of Tertiary mafic alkaline magmas in the Hocheifel, Germany. *Journal of Petrology* 47, 1637–1671. https://doi.org/10.1093/petrology/egl023

Jung S. 1995: Geochemistry and petrogenesis of rift-related Tertiary alkaline rocks from the Rhön area (central Germany). *Neues Jahrbuch für Mineralogie Abhandlungen* 169, 193–226.

Jung S., Mezger K., Nebel O., Kooijman E., Berndt J., Hauff F. & Münker C. 2012: Origin of Meso-Proterozoic post-collisional leucogranite suites (Kaokoveld, Namibia): constraints from geochronology and Nd, Sr, Hf, and Pb isotopes. *Contributions to Mineralogy and Petrology* 163, 1–17. https://doi.org/10.1007/s00410-011-0655-y

Jung S., Mezger K., Hauff F., Pack A. & Hoernes S. 2013: Petrogenesis of rift-related tephrites, phonolites and trachytes (Central European Volcanic Province, Rhön, FRG): Constraints from Sr, Nd, Pb and O isotopes. *Chemical Geology* 354, 203–215. https://doi.org/10.1016/j.chemgeo.2013.06.026

Keppler H. 1996: Constraints from partitioning experiments on the composition of subduction-zone fluids. *Nature* 380, 237–240. https://doi.org/10.1038/380237a0

Kolb M., Paulick H., Kirchenbaur M. & Münker C. 2012: Petrogenesis of mafic to felsic lavas from the Oligocene Siebengebirge volcanic field (Germany): implications for the origin of intracontinental volcanism in Central Europe. *Journal of Petrology* 53, 2349–2379. https://doi.org/10.1093/petrology/egs053

Krausová I., Mizera J., Řanda Z., Chvátil D. & Krist P. 2015: Non-destructive assay of fluorine in geological and other materials by instrumental photon activation analysis with a microtron. *Nuclear Instruments and Methods in Physics Research Section B* 342, 82–86. https://doi.org/10.1016/j.nimb.2014.09.023

Krmíček L., Ulrych J., Šišková P., Krmíčková S., Špaček P. & Křížová Š. 2020: Geochemistry and Sr–Nd–Pb isotope characteristics of Miocene basalt–trachyte rock association in transitional zone between the Outer Western Carpathians and Bohemian Massif. *Geologica Carpathica* 71, 462–482. https://doi.org/10.31577/GeolCarp.71.5.6

Krmíček L., Ulrych J., Jelínek E., Skála R., Krmíčková S., Korbelová Z. & Balogh K. 2021: Petrogenesis of Cenozoic high-Mg (picritic) volcanic rocks in the České středohoří Mts. (Bohemian Massif, Czech Republic). *Mineralogy and Petrology* 115, 193–211. https://doi.org/10.1007/s00710-020-00729-5

Krmíčková S., Krmíček L., Romer R.L. & Ulrych J. 2020: Lead isotope evolution of the Central European upper mantle: Constraints from the Bohemian Massif. *Geoscience Frontiers* 11, 925–942. https://doi.org/10.1016/j.gsf.2019.09.009

Kühn J. 1990: Geochemistry of trachytic rocks of the Lužické hory Mts. *Charles University*, Prague, 1–142.

Laporte D., Lambart S., Schiano P. & Ottolini L. 2014: Experimental derivation of nepheline syenite and phonolite liquids by partial melting of upper mantle peridotites. *Earth and Planetary Science Letters* 404, 319–331. https://doi.org/10.1016/j.epsl.2014.08.002

Le Bas M.J. 1987: Nephelinites and carbonatites. *Geological Society, London, Special Publications* 30, 53–83. https://doi.org/10.1144/GSL.SP.1987.030.01.05

Le Maitre R.W. 2002: Igneous Rocks. A Classification and Glossary of Terms. *Cambridge University Press*, Cambridge, 1–236. https://doi.org/10.1017/CBO9780511535581

Le Roex A.P., Cliff R.A. & Adair B.J.I. 1990: Tristan da Cunha, South Atlantic: geochemistry and petrogenesis of a basanite–phonolite lava series. *Journal of Petrology* 31, 779–812. https://doi.org/10.1093/petrology/31.4.779

Legendre C., Maury R.C., Caroff M., Guillou H., Cotton J., Chauvel C., Bollinger C., Hémond C., Guille G., Blais S., Rossi P. & Savanier D. 2005: Origin of exceptionally abundant phonolites on Ua Pou Island (Marquesas, French Polynesia): partial melting of basanites followed by crustal contamination. *Journal of Petrology* 46, 1925–1962. https://doi.org/10.1093/petrology/egi043

Lexa J., Seghedi I., Németh K., Szakács A., Konečný V., Pécskay Z., Fülöp A. & Kovacs M. 2010: Neogene-Quaternary volcanic forms in the Carpathian-Pannonian Region: a review. *Open Geosciences* 2, 207–270. https://doi.org/10.2478/v10085-010-0024-5

Lustrino M. & Wilson M. 2007: The circum-Mediterranean anorogenic Cenozoic igneous province. *Earth-Science Reviews* 81, 1–65. https://doi.org/10.1016/j.earscirev.2006.09.002

Macdonald R. 2003: Magmatism of the Kenya Rift Valley: a review. *Transactions of the Royal Society of Edinburgh: Earth Sciences* 93, 239–253. https://doi.org/10.1017/S0263593300000420

Macdonald R. & Scaillet B. 2006: The central Kenya peralkaline province: Insights into the evolution of peralkaline salic magmas. *Lithos* 91, 59–73. https://doi.org/10.1016/j.lithos.2006.03.009

Maciotta G., Almeida A., Barbieri M., Beccaluva L., Gomes C., Morbidelli L., Ruberti E., Siena F. & Traversa G. 1990: Petrology of the tephrite/phonolite suite and cognate xenoliths of the Fortaleza district (Ceará, Brazil). *European Journal of Mineralogy* 2, 687–709.

Mayer B., Jung S., Romer R.L., Stracke A., Haase K.M. & Garbe-Schönberg C.D. 2013: Petrogenesis of Tertiary hornblende-bearing lavas in the Rhön, Germany. *Journal of Petrology* 54, 2095–2123. https://doi.org/10.1093/petrology/egt042

McDonough W.F. & Sun S.S. 1995: The composition of the Earth. *Chemical Geology* 120, 223–253. https://doi.org/10.1016/0009-2541(94)00140-4

McLennan S.M. 1989: Rare earth elements in sedimentary rocks: influence of provenance and sedimentary processes. *Reviews in Mineralogy and Geochemistry* 21, 169–200. https://doi.org/10.1515/9781501509032-010

Menzies M.A. 1983: Mantle ultramafic xenoliths in alkaline magmas: evidence for mantle heterogeneity modified by magmatic activity. In: Hawkesworth C.J. & Norry M.J. (Eds.): Continental basalts and mantle xenoliths. *Shiva Publishing*, Nantwich, 92–110.

Merlet C. 1992: Quantitative electron probe microanalysis: new accurate Φ (ρz) description. *Microchimica Acta* 12, 107–115. https://doi.org/10.1007/978-3-7091-6679-6_8

Meyer R. & Foulger G.R. 2007: The European Cenozoic Volcanic Province is not caused by mantle plumes. *MantlePlumes.org.* Available online: www.mantleplumes.org/Europe.html (accessed September 1, 2025).

Mikysek P., Zikmund T., Dosbaba M., Břínek A., Slobodník M., Adamovič J., Mészárosová N., Trojek T. & Kaiser J. 2021: Multi-scale visualization of uranium-rich domains dispersed in U–Zr mineralization of sandstone-type (Břevniště, Czech Republic). *Ore Geology Reviews* 138, 104358. https://doi.org/10.1016/j.oregeorev.2021.104358

Mizera J. & Řanda Z. 2010: Instrumental neutron and photon activation analyses of selected geochemical reference materials. *Journal of Radioanalytical and Nuclear Chemistry* 284, 157–163. https://doi.org/10.1007/s10967-010-0447-2

Morimoto N., Fabries J., Ferguson A.K., Ginzburg I.V., Ross M., Seifert F.A., Zussman J., Aoki K. & Gottardi G. 1988: Nomenclature of pyroxenes. *American Mineralogist* 73, 1123–1133.

Odin G.S. 1982: Interlaboratory standards for dating purposes. In: Odin G.S. (Ed.): Numerical Dating in Stratigraphy. *Wiley & Sons*, New York, 123–149.

Panter K.S., Blusztajn J., Hart S.R., Kyle P.R., Esser R. & McIntosh W.C. 2006: The origin of HIMU in the SW Pacific: evidence from intraplate volcanism in southern New Zealand and subantarctic islands. *Journal of Petrology* 47, 1673–1704. https://doi.org/10.1093/petrology/egl024

Panter K.S., Kyle P.R. & Smellie J.L. 1997: Petrogenesis of a phonolite–trachyte succession at Mount Sidley, Marie Byrd Land, Antarctica. *Journal of Petrology* 38, 1225–1253. https://doi.org/10.1093/petroj/38.9.1225

Papanastassiou D.A. & Wasserburg G.J. 1969: Initial strontium isotopic abundances and the resolution of small time differences in the formation of planetary objects. *Earth and Planetary Science Letters* 5, 361–376. https://doi.org/10.1016/S0012-821X(68)80066-4

Pazdernik P. 1997: Compositional variations in the sodalite-bearing nepheline syenite from Želenický vrch Hill, North Bohemia. *Acta Universitatis Carolinae: Geologica* 41, 65–79.

Pazdernik P. 1998: Phonolitic and trachytic rocks in the České středohoří Mts., North Bohemia: Petrology and geochemistry. In: Novák M. & Rosenbaum J. (Eds.): Challenges to Chemical Geology: Refereed Papers from MAEGS-10. *Czech Geological Survey*, Prague, 93–101.

Pfänder J.A., Jung S., Klügel A., Münker C., Romer R.L., Sperner B. & Rohrmüller J. 2018: Recurrent local melting of metasomatised lithospheric mantle in response to continental rifting: Constraints from basanites and nephelinites/melilitites from SE Germany. *Journal of Petrology* 59, 667–694. https://doi.org/10.1093/petrology/egy041

Pin C., Gannoun A. & Dupont A. 2014: Rapid, simultaneous separation of Sr, Pb, and Nd by extraction chromatography prior to isotope ratios determination by TIMS and MC-ICP-MS. *Journal of Analytical Atomic Spectrometry* 29, 1858–1870. https://doi.org/10.1039/C4JA00169A

Pivec E., Ulrych J. & Langrová A. 2004: On the origin of pseudoleucite from Cenozoic phonolite dyke from Loučná/Böhmisch Oberwiesenthal, Krušné hory/Erzgebirge Mts., Bohemia. *Neues Jahrbuch für Mineralogie Abhandlungen* 179, 221–238. https://doi.org/10.1127/0077-7757/2004/0179-0221

Pontesilli A., Brenna M., Mollo S., Masotta M., Nazzari M., Le Roux P. & Scarlato P. 2022: Trachyte-phonolite transition at Dunedin Volcano: Fingerprints of magma plumbing system maturity and mush evolution. *Lithos* 408, 106545. https://doi.org/10.1016/j.lithos.2021.106545

Potts P.J. 1995: A Handbook of Silicate Rock Analysis. *Blackie Academic and Professional*, London, 1–622.

Rudnick R.L. & Gao S. 2014: Composition of the continental crust. In: Holland H. & Turekian K. (Eds.): Treatise on Geochemistry, Volume 4. *Elsevier*, Amsterdam, 1–51. https://doi.org/10.1016/B978-0-08-095975-7.00301-6

Řanda Z., Frána J., Mizera J., Kučera J., Novák J.K., Ulrych J., Belov A.G. & Maslov O.D. 2007: Instrumental Neutron and Photon Activation Analysis in the Geochemical Study of Phonolitic and Trachytic Rocks. *Geostandards and Geoanalytical Research* 31, 275–283. https://doi.org/10.1111/j.1751-908X.2007.00839.x

Salters V.J., Longhi J.E. & Bizimis M. 2002: Near mantle solidus trace element partitioning at pressures up to 3.4 GPa. *Geochemistry, Geophysics, Geosystems* 3, 1–23. https://doi.org/10.1029/2001GC000148

Schleicher H., Keller J. & Kramm U. 1990: Isotope studies on alkaline volcanics and carbonatites from the Kaiserstuhl, Federal Republic of Germany. *Lithos* 26, 21–35. https://doi.org/10.1016/0024-4937(90)90038-3

Schleicher H., Baumann A. & Keller J. 1991: Pb isotopic systematics of alkaline volcanic rocks and carbonatites from the Kaiserstuhl, upper Rhine rift valley, FRG. *Chemical Geology* 93, 231–243. https://doi.org/10.1016/0009-2541(91)90116-9

Schreiber U., Anders D. & Koppen J. 1999: Mixing and chemical interdiffusion of trachytic and latitic magma in a subvolcanic complex of the Tertiary Westerwald (Germany). *Lithos* 46, 695–714. https://doi.org/10.1016/S0024-4937(98)00091-7

Shrbený O. 1989: Major and trace elements in Tertiary volcanics of the Lužické hory Mts. and the adjacent area, northern Bohemia. *Journal of Mineralogy and Geology* 34, 235–253.

Skála R., Ulrych J., Böhmová V., Korbelová Z. & Novák J.K. 2010: Zirconium-bearing minerals in phonolites of northern Bohemia. *Acta Mineralogica-Petrographica, Abstract Series* 6, 461.

Skála R., Ulrych J., Ackerman L., Krmíček L., Fediuk F., Balogh K. & Hegner E. 2015: Upper Cretaceous to Pleistocene melilitic volcanic rocks of the Bohemian Massif: petrology and mineral chemistry. *Geologica Carpathica* 66, 197–216. https://doi.org/10.1515/geoca-2015-0020

Strnad L., Mihaljevič M. & Šebek O. 2005: Laser ablation and solution ICP-MS determination of rare earth elements in USGS BIR-1G, BHVO-2G and BCR-2G glass reference material. *Geostandards and Geoanalytical Research* 29, 303–314. https://doi.org/10.1111/j.1751-908X.2005.tb00902.x

Sun S. 1982: Chemical composition and origin of the Earth's primitive mantle. *Geochimica et Cosmochimica Acta* 46, 179–192. https://doi.org/10.1016/0016-7037(82)90245-9

Sun S. & Mc Donough W.F. 1989: Chemical and isotopic systematics of oceanic basalts. Implication for mantle composition and processes. *Geological Society, London, Special Publications* 42, 313–345. https://doi.org/10.1144/GSL.SP.1989.042.01.19

Szakács A., Pécskay Z. & Gál Á. 2018: Patterns and trends of time–space evolution of Neogene volcanism in the Carpathian–Pannonian region: a review. *Acta Geodaetica et Geophysica* 53, 347–367. https://doi.org/10.1007/s40328-018-0230-3

Todt W., Cliff R.A., Hanser A. & Hofmann A.W. 1996: Evaluation of a ^{202}Pb–^{205}Pb Double Spike for High-Precision Lead Isotope Analysis. *Geophysical Monograph Series* 95, 429–437. https://doi.org/10.1029/GM095p0429

Ulrych J. & Pivec E. 1997: Age-related contrasting alkaline volcanic series in North Bohemia. *Chemie der Erde* 57, 311–336.

Ulrych J., Pivec E., Rychlý R. & Rutšek J. 1992: Zirconium mineralization of young alkaline volcanic rocks from northern Bohemia. *Geologica Carpathica* 43, 91–95.

Ulrych J., Pivec E., Höhndorf A., Balogh K., Bendl J. & Rutšek J. 2000a: Rhyolites from the Roztoky Intrusive Centre, České středohoří Mts.: xenoliths or dyke differentiates? *Chemie der Erde* 60, 327–352.

Ulrych J., Pivec E., Lang M. & Lloyd F.E. 2000b: Ijolitic segregations in melilite nephelinite of Podhorní vrch volcano, Western Bohemia. *Neues Jahrbuch für Mineralogie Abhandlungen* 175, 317–348. https://doi.org/10.1127/njma/175/2000/317

Ulrych J., Svobodová J. & Balogh K. 2002: The source of Cenozoic volcanism in the České středohoří Mts., Bohemian Massif. *Neues Jahrbuch für Mineralogie Abhandlungen* 177, 133–162. https://doi.org/10.1127/0077-7757/2002/0177-0133

Ulrych J., Lloyd F.E., Balogh K., Hegner E., Langrová A., Lang M., Novák J.K. & Řanda Z. 2005: Petrogenesis of alkali pyroxenite and ijolite xenoliths from the Tertiary Loučná-Oberwiesenthal Volcanic Centre, Bohemian Massif in the light of new mineralogical, geochemical and isotopic data. *Neues Jahrbuch für Mineralogie Abhandlungen* 182, 57–79. https://doi.org/10.1127/0077-7757/2005/0029

Ulrych J., Dostal J., Adamovič J., Jelínek E., Špaček P., Hegner P. & Balogh K. 2011: Recurrent Cenozoic volcanic activity in the Bohemian Massif (Czech Republic). *Lithos* 123, 133–144. https://doi.org/10.1016/j.lithos.2010.12.008

Ulrych J., Adamovič J., Krmíček L., Ackerman L. & Balogh K. 2014: Revision of Scheumann's classification of melilitic lamprophyres and related melilitic rocks in light of new analytical data. *Journal of Geosciences* 59, 3–22. https://doi.org/10.3190/jgeosci.158

Ulrych J., Krmíček L., Tomek Č., Lloyd F.E., Ladenberger A., Ackerman L., Balogh K. 2016: Petrogenesis of Miocene alkaline volcanic suites from western Bohemia: whole rock geochemistry and Sr–Nd–Pb isotopic signatures. *Chemie der Erde* 79, 77–93. https://doi.org/10.1016/j.chemer.2015.11.003

Ulrych J., Krmíček L., Adamovič J. & Krmíčková S. 2022: The story of post-Variscan lamprophyres of the Bohemian Massif: from ultramafic (Upper Cretaceous–Paleocene) to alkaline (Eocene–Oligocene) types. *Geological Society, London, Special Publications* 513, 237–269. https://doi.org/10.1144/SP513-2020-233

Upton G.G.J., Stephenson D. & Ellam R.M. 2007: Silica-undersaturated trachytic rocks of central Scotland. *Scottish Journal of Geology* 43, 143–153. https://doi.org/10.1144/sjg43020143

Vaněčková M., Holub F., Souček J. & Bowes D.R. 1993: Geochemistry and petrogenesis of the Tertiary alkaline volcanic suite of the Labe tectono-volcanic zone, Czech Republic. *Mineralogy and Petrology* 48, 17–37. https://doi.org/10.1007/BF01164906

Warr L.N. 2021: IMA–CNMNC approved mineral symbols. *Mineralogical Magazine* 85, 291–320. https://doi.org/10.1180/mgm.2021.43

Watson E.B. 1979: Zirconium-saturation in felsic liquids: experimental results and application to trace element geochemistry. *Contributions to Mineralogy and Petrology* 70, 409–419. https://doi.org/10.1007/BF00371047

Wedepohl K.H., Gohn E. & Hartmann G. 1994: Cenozoic alkali basalt magmas of western Germany and their products of differentiation. *Contributions to Mineralogy and Petrology* 115, 253–278. https://doi.org/10.1007/BF00310766

Wenger E., Büchner J., Tietz O. & Mrlina J. 2017: The polycyclic Lausche volcano (Lausitz volcanic field) and its message concerning landscape evolution in the Lausitz mountains (northern Bohemian Massif, central Europe). *Geomorphology* 292, 193–210. https://doi.org/10.1016/j.geomorph.2017.04.021

Wiesmaier S., Troll V.R., Carracedo J.C., Ellam R.M., Bindeman I., Wolff J.A. & Deegan F.M. 2013: Magmatic Differentiation in the Teide–Pico Viejo Succession: Isotope Analysis as a Key to Deciphering the Origin of Phonolite Magma. In: Carracedo J.C. & Troll V.R. (Eds.): Teide Volcano. *Springer*, Berlin, 173–190. https://doi.org/10.1007/978-3-642-25893-0_10

Wilson M. & Bianchini G. 1999: Tertiary–Quaternary magmatism within the Mediterranean and surrounding regions. *Geological Society, London, Special Publications* 156, 141–168. https://doi.org/10.1144/GSL.SP.1999.156.01.09

Wilson M. & Downes H. 1991: Tertiary–Quaternary extension-related alkaline magmatism in western and central Europe. *Journal of Petrology* 32, 811–849. https://doi.org/10.1093/petrology/32.4.811

Wilson M., Downes H. & Cebrià J.H. 1995: Contrasting fractionation trends in coexisting continental alkaline magma series; Cantal, Massif Central, France. *Journal of Petrology* 36, 1729–1753. https://doi.org/10.1093/oxfordjournals.petrology.a037272

Wörner G., Beusen J.M., Duchateau N., Gijbels R. & Schmincke H.U. 1983: Trace element abundances and mineral/melt distribution coefficients in phonolites from the Laacher See Volcano (Germany). *Contributions to Mineralogy and Petrology* 84, 152–173. https://doi.org/10.1007/BF00371282

Wörner G., Staudigel H. & Zindler A. 1985: Isotopic constraints on open system evolution of the Laacher See magma chamber (Eifel, West Germany). *Earth and Planetary Science Letters* 75, 37–49. https://doi.org/10.1016/0012-821X(85)90048-2

Wörner G., Zindler A., Staudigel H. & Schmincke H.U. 1986: Sr, Nd, and Pb isotope geochemistry of Tertiary and Quaternary alkaline volcanics from West Germany. *Earth and Planetary Science Letters* 79, 107–119. https://doi.org/10.1016/0012-821X(86)90044-0

Zartman R.E. & Doe B.R. 1981: Plumbotectonics – the model. *Tectonophysics* 75, 135–162. https://doi.org/10.1016/0040-1951(81)90213-4

Ziegler P.A. 1994: Cenozoic rift system of Western and Central Europe: an overview. *Geologie en Mijnbouw* 73, 99–127.

Zindler A. & Hart S. 1986: Chemical geodynamics. *Annual Review of Earth and Planetary Sciences* 14, 493–571. https://doi.org/10.1146/annurev.ea.14.050186.002425

Electronic supplementary material is available online:
Supplement S1 at https://geologicacarpathica.com/data/files/supplements/GC-76-5-Krmickova_SupplS1.xlsx
Supplement S2 at https://geologicacarpathica.com/data/files/supplements/GC-76-5-Krmickova_SupplS2.xlsx